NKS-352
ISBN 978-87-7893-436-9

Advanced In-situ Gamma Spectrometry Field Activity – Chernobyl (GAMFAC)

M. Dowdall[1], Yu. Bondar[2], P. Fristrup[3], K. Guðnason[5], M. Granström[4]
A. Hedman[4], C. Israelson[3], G. Jónsson[5], S. Kjerulf[3], S. Juul Krogh[3]
A. Mauring[1], B. Moller[1], A. Tyler[6], A. Varley[6], V.Zabrotski[2]

[1] Norwegian Radiation Protection Authority, Norway
[2] Polessie State Radiation-Ecological Reserve, Belarus
[3] Danish Emergency Management Agency, Denmark
[4] FOI, Swedish Defence Research Agency, Sweden
[5] Icelandic Radiation Safety Authority, Iceland.
[6] University of Stirling, United Kingdom.

November 2015

Abstract

The GAMFAC activity provided an opportunity for the testing of equipment, procedures and personnel in conducting in-situ measurements in areas of high contamination with complex confounding factors. The activity was conducted within the confines of the Belarusian Exclusion Zone during the autumn of 2015 in collaboration with the Polessie State Radiation Ecology Reserve (PSRER) who administer the Belarusian Exclusion Zone. Five teams from the Nordic countries utilising a range of in-situ measurement equipment spent 5 days making a series of measurements at a number of pre-selected and pre-characterised sites varying in terms of contamination density, topography, pedological properties etc. Detailed information was available as to contamination density, depth distribution, soil characteristics etc. A wide range of equipment was available for the activity ranging from small CDZnTe detectors to larger detectors of conventional materials including HPGe and NaI/LaBr. A range of calibration methods had been used, in addition to a broad selection of procedures adopted by the teams during the activity. The use of common sites for the making of measurements by the teams facilitated intercomparison of methods and equipment while he availability of detailed laboratory measurements allowed for optimal adjustment of equipment and analysis parameters. The GAMFAC report presents a background to and overview of the activity. Detailed descriptions of equipment and procedures are included as well as detailed analysis of results.

Key words

In-situ gamma ray spectrometry, Belarus, Chernobyl, Exclusion Zone.

NKS-352
ISBN 978-87-7893-436-9
Electronic report, November 2015
NKS Secretariat
P.O. Box 49
DK - 4000 Roskilde, Denmark
Phone +45 4677 4041
www.nks.org
e-mail nks@nks.org

Table of Contents

ACKNOWLEDGEMENTS

The authors wish to acknowledge the NKS, the participating organisations, Elena Almås and the staff of the Polessie State Radiation Ecology Reserve of Belarus for their invaluable support in the GAMFAC activity.

DISCLAIMER

The mentioning of equipment, production companies, instruments, software or other tradenames does not constitute an endorsement on the part of NKS, participating teams or their institutions.

1.0 Introduction

In-situ gamma spectrometry can be a cost effective, rapid, practicable means of assessing radioactive contamination in contaminated environments. While relatively simple in application at first glance, full and effective exploitation of the method requires careful consideration of a range of factors which increase in complexity as one moves farther away from the elementary case of, for example, ^{137}Cs evenly deposited on a uniform flat surface. Unven contamination distribution with depth, matrices that vary in topography and physico-chemical properties, the presence of other nuclides, heterogenous deposition etc. can serve to significantly complicate the generation of reliable, robust data from the technique. In-situ gamma spectrometry has undergone significant developments in recent years in terms of both hardware and software and these developments have precipitated an increased penetration of the method into the analytical arsenals of a number of Nordic countries. From a Nordic perspective, the environment within which these analytical tools are typically deployed is relative homogenous – Chernobyl ^{137}Cs deposited in relatively similar natural environments which have been subject to similar environmental processes since the time of deposition. This homogeneity, in both the character of the deposition and the experience of in-situ gamma spectrometry, has arguably functioned as a restrictive boundary for the further maturation of in-situ analytical capabilities in the Nordic region. Whilst the current application of such techniques is probably sufficient for the extant situation, the realisation of the full potential of such techniques requires a shift in the boundaries imposed by the Nordic context. While activities such as NKS MOMS have served to focus attention on the potential usefulness of such methods, experience can only be gained and improvements can only be made through the practical application of the methods in environments or contexts that facilitate the generation of useful data under conditions that stretch the capabilities of both the equipment and the operator. In addition, although seminars and workshops provide valuable exposure to the current state of the art in such techniques, their full value can only be appreciated through observation and implementation of them in practice.

In-situ methods, in addition to mobile measurements, constitute one of the first sources of information in the event of a nuclear accident resulting in deposition of radioactive contaminants. As such, a strong case can be made for ensuring the robustness and reliability of data that may be generated in, and subsequently shared between, the countries of the Nordic region. Demonstrations of capabilities and comparability of results generated in different countries are important measures in establishing confident responses to nuclear

accidents and incidents and ensuring demonstrability of the quality of generated data. While such matters can most likely be effectively handled for the post-Chernobyl Nordic situation, robustness and comparability for possible future situations are difficult to demonstrate without actually conducting such measurements in an environment that can serve to represent conditions that may exist in the aftermath of a significant accident. In-situ measurements are part of an analytical suite that have come to preponderence in the years after the Chernobyl accident. Practitioners of such methods are, in many cases, a generation of operatives who started their careers in the years after the Chernobyl accident and many have never witnessed the types or levels of contamination that can result from an accident. In this regard, the importance of exposing operatives to conditions that represent the aftermath of an accident and the technical difficulties that may be imposed should not be underestimated. In addition, the last decade has seen a profusion of methods for the determination of response functions for in-situ detectors based around mathematical methods as opposed to direct empirical measurement. Various Monte Carlo suites and software packages employing deterministic methods have been used to establish calibrations for in-situ measurement systems and have been used to appraise and correct for the effects of such aspects as depth distributions of isotopes in the soil column and variations in soil types and matrices. The GAMFAC activity provides an ideal opportunity for the testing of such methods in the field and will facilitate the exchange of abilities and experience with such methods between the participating teams.

Bearing in mind the above, the intention of NKS GAMFAC was to address as many of the above considerations with one activity – a practical field operation involving an area significantly contaminated by more than just ^{137}Cs with environmental conditions different to those in the Nordic region where the full suite of challenges in making robust, dependable in-situ measurements are represented. For the purpose of added value and to build upon the experience from NKS MOMS, the field activity was be conducted in cooperation with a recognised international expert in the area of in-situ gamma spectrometry who has previously served as a guest speaker in NKS activities, thereby providing a valuable practical exposure to the latest methods and developments for the participating teams.

The primary objective of the GAMFAC activity was: "*the provision of a technically challenging intercomparison and experience exchange field activity in the area of in-situ gamma spectrometry*" . Secondary, but equally important, objectives included the provision of calibration opportunities, the development and testing of new techniques for expanding the

Nordic capabilities in in-situ gamma spectromery, conducting field operations with recognised experts in the field, pushing the boundaries of the usual Nordic experience of "just ^{137}Cs", establishing and building upon extant Nordic networks in the area of in-situ gamma spectrometry, increasing the functionality and application range of in-situ gamma spectrometry, improving the rapid response capabilities of Nordic operatives in international assisstance situations and ensuring demonstrable comparability between in-situ measurements conducted in the Nordic countries.

These objectives were fulfilled through an NKS funded, joint Nordic field activity in the Belarusian Exclusion Zone conducted in collaboration with an invited international expert in the field of in-situ gamma spectrometry. In order to avoid directionless effort, the activity was carefully planned in advance with the Belarusian authorities on the ground such that maximum benefit could be accrued via an efficient usage of the time and resources available. In addition to the direct objectives listed above, the proposed activity built further upon relations already established between the Nordic countries and Belarus and served as a useful and efficient means of conducting technical exchange between the responsible authorities in Belarus and counterparts in the Nordic countries in a matter of some import in regards to emergency preparedness and response.

2.0 The Belarusian Exclusion Zone

The most contaminated regions in Belarus occur in the southern reaches of the Gomel Region along the border with the Ukraine, the Belarusian exclusion zone beginning just south of the town of Khoiniki. The most contaminated areas are sealed off from public access and now function as a scientific nature reserve. All entry to and activities within these areas are strictly controlled by the relevant authorities. An approximate indication of the controlled zone is provided in Figure 1 including the main settlements in the area. Heaviest contamination, in excess of 1.4 MBq/m^2 of ^{137}Cs is found in the southernmost parts of the zone nearest the reactor (the reactor is, at its closest, some kilometers from the southernmost extent of the Belarusian zone and is visible over the trees in places) although patches of high contamination can be found in many places throughout the zone. Significant amounts of ^{90}Sr are also present (up to 3 MBq/m^2) with some ^{241}Am (which has approximately doubled in concentration of the past twenty years, currently of the order of up to 100 kBq/m^2), actinides (^{238}Pu up to 37 kBq/m^2; ^{239,240}Pu up to 74 kBq/m^2) and in places ^{154}Eu. Estimates indicate that approximately

1/3 of the radiocesium and 70% of the strontium released from Chernobyl ended up on the territories of the the PSRER.

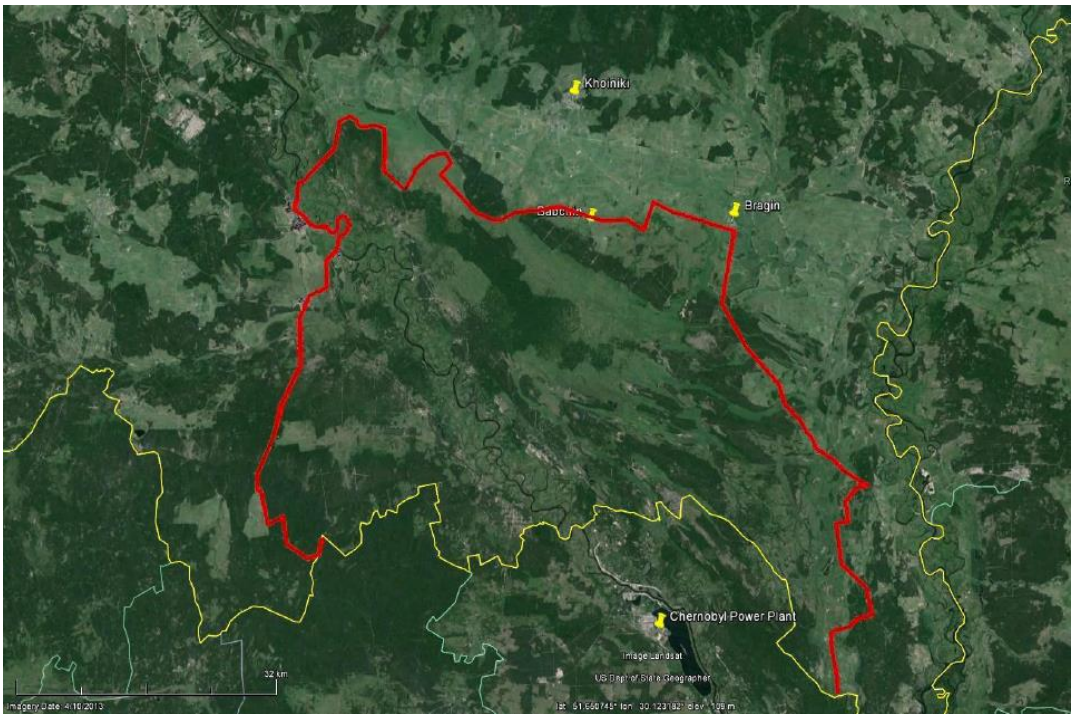

Figure 1. *The extent of the PSRER, delineated in red, and major settlements. The location of the Ukrainian- Belarus border is also indicated as well as the location of the Chernobyl power plant.*

The broad picture of the contamination pattern in relation to ^{137}Cs is given in Figure 2. On a local scale, the contamination is highly heterogenous (over scales of 10's of meters or less). Significant contamination is also present in the tree canopy and above ground vegetation, in water bodies and courses and in sediments therof.

The regulations of the Central Committee CPB and Council of Ministers of BSSR № 59-5 from February, 24th, 1988 established a nature reserve on the land of the Belarusian sector within a 30-km zone of the Chernobyl NPP. The reserve commenced operations in September, 1988 after the order № 354-p from August, 23rd, 1988 by Gomel District Executive Committee "*About the formation of temporal administration of the Polessian state ecological nature reserve*". It initially consisted of 131.3 thousand hectares and was managed by the State Committee on Ecology of the Republic of Belarus.

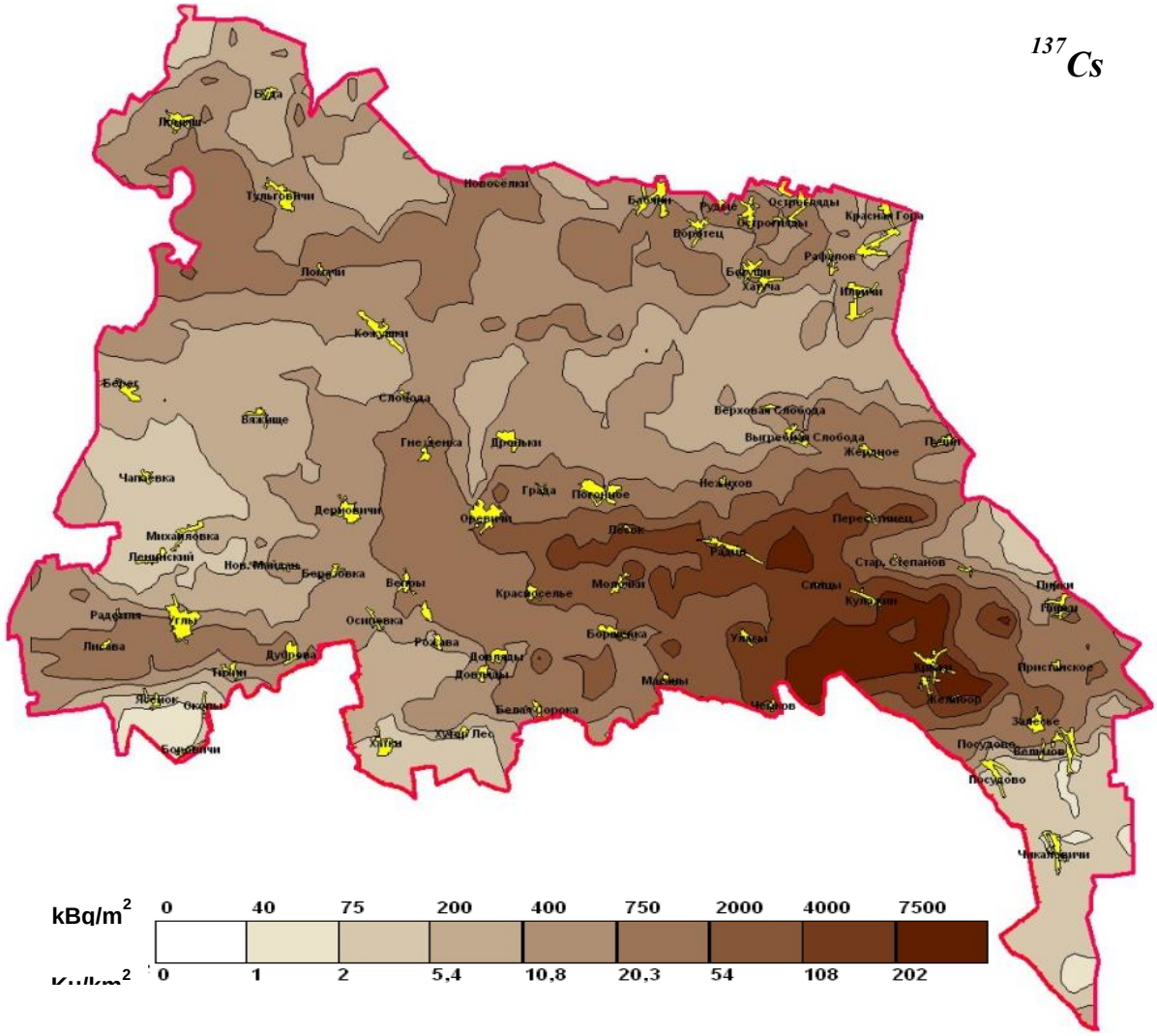

Figure 2. Distribution of ^{137}Cs within the territory of the Belarusian Exclusion Zone as of 2011.

The regulation of the Council of Ministers of Belarus № 122 from February, 10th, 1989 renamed it to the Polessian State Radiation-Ecological Reserve (PSRER) which at the present is managed by the Department for Liquidation of the Consequences of the Accident at the Chernobyl NPP of the Ministry of Emergency Measures of Belarus. In 1993 the PSRER was expanded to include 84.8 thousand more hectares of land and its area then made up a total of 216.2 thousand hectares. Administratively it occupies part of the Hoyniksky, Braginsky and Narovlyansky areas of the Gomel district which earlier had 92 settlements, now all abandoned. It is structurally divided into three distinct sites located on the territories of the corresponding areas and 16 forest areas.

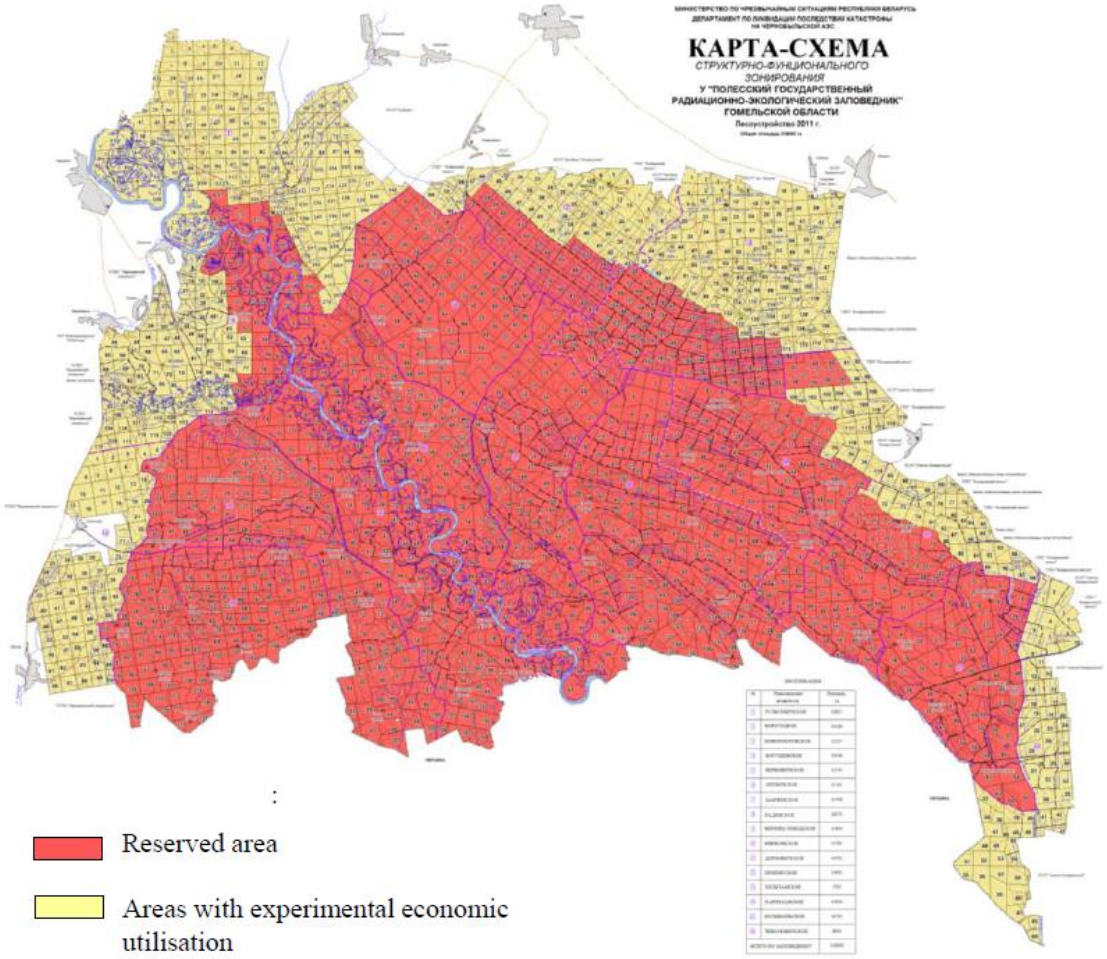

Figure 3. *Division of the PSRER into areas of totally restricted access and areas where trial schemes regarding economic activity take place.*

The Belarusian zone is managed by the staff of the reserve. This entity is responsible for managing the zone, controlling entry, conducting scientific research etc. It has a workforce that is probably approaches 700 and answers to the Ministry of Emergency Measures. They have their main base within the zone at a facility called Babchin as well as operating two other similar facilities and a number of research and fire stations much farther into the zone itself. The reserve also operates some experimental farms and other sites which function to serve the authorities initiatives in trying to investigate possible uses for the zone. The Babchin facility includes laboratories, workshops and administrative facilities for the staff as well as basic overnighting facilities for the staff and a canteen. There is also a museum and other things.

The primary goals of the PSRER in their management of the zone are:

- Protection of the territory from unauthorized entry and fire prevention;
- Measures to prevent the spread of radionuclides to adjoining areas,
- Radioecological monitoring of land, air, water, flora and fauna;
- Research on the influence of radioactive pollution on flora and fauna,
- Afforestation of the land, primarily those subject to wind and water erosion.

Twelve control posts exist within the zone, manned on a 24 hour basis for the purpose of protection of the territory from unauthorized entries. All perimeters and access points are manned and patrolled. Warning notices and barriers are visible on the perimeter of the reserve and on roads approaching too and within the zone. Warning signs as to areas of heavy contamination can be found within the zone although the accuracy of some of them, given their age, is unclear. Extensive fire prevention measures have been constructed and fire protection consists of firebreaks and observation posts. Approximately 155 km of firebreaks with a width of 40 m, 200 km with a width width of 15 m and 1440 km of deforested mineralized zones have been created to hinder fire spreading. Some 99 artificial water reservoirs have been created to assist fire fighting and 37 observation towers have been established in order to monitor for fire outbreaks.

Staff of the PSRER are subject to special regulation in relation to restriction of the time they may spend in the zone, the useage of personal radiation monitoring devices, individual control regimes for exzternal and internal exposure, decontamination procedures for personnel and vehicles and health checks.

The PSRER is located in a subzone of foliar and pine woods, forested areas making up 109.7 thousand hectares (51.1 % of the territory) of which pine woods constitute 43.9 % of the afforested areas, birch woods 30.7 %, black alder 12.4 %, oak 6.3 % and other species 6.7 %. The territories not covered by woods (basically abandoned agricultural lands) constitute 82.2 thousand hectares (38.0 %) and non-agricultural unforested lands occupy 20.1 thousand hectares (9.3 %).

Figure 4. *Representation of some of the various landscape types found within the territory of the PSRER.*

Some 884 species of vascular plants are found in the territory including a high number of rare and protected species. Over 60 species of mammal can be found in Belarus, 46 species being found in the PSRER. These species include 6 of the 7 red listed species found in Belarus and include brown bear, lynx, wolf and European bison. Przewalski horses have been regularly observed since 2007.The three scientific departments of the PSRER cover radioecological monitoring, the ecology of vegetation, the ecology of fauna and a laboratory for spectrometry and radiochemistry. The laboratory of spectrometry and radiochemistry is accredited according to the requirements STB ISO/MEK 17025 since 2005. The PSRER also conducts studies into possible methods for the rehabilitation of the contaminated zone. These investigations include the construction of an experimental bee apiary and gardens and a horse breeding programme initiated in 1996.

The topography of the area is reasonably flat and even, small elevations and depressions being encountered locally. Small abandoned villages and buildings are encountered along the

road but are in the main largely dominated by surrounding vegetation and trees. Numerous water features are present both beside and under the roads in places. These consist largely of small streams, rivers, drainage and irrigation channels, flooded areas and small lakes and swamps. Forested areas are present throughout the reserve – comprised of managed plantations on the peripherery of the reserve (see Figure 3) and more natural stands of trees in the interior. In all areas extensive and wide firebreaks have been constructed, the exposed overburden along these breaks being mostly vegetation free and consisting of exposed or deposited sand. There are essentially no visible outcrops of the underlying geology and few buildings constructed of natural stone in the vicinity of the roads. Some parts of the reserve, in particular near research stations in the interior have been modified by having the upper layers of soil removed to reduce ambient dose rates but these modifications are primarily confined to the immediate surroundings of these facilities.

3.0 The GAMFAC Activity

The following section otlines how the GAMFAC was conducted on a practical level, arrangements made on the ground for achieving the objectives of the activity, the teams participating, the equipment deployed and the analytical and calibration procedures implemented.

3.1 The Participating Teams

3.1.1 Norwegian Radiation Protection Authority, Norway

The NRPA operated two independent spectrometric detector systems during the activity. Both systems are shown in Figure 5. The main set-up comprises a GR1-A+ detector manufactured by Kromek (UK) connected to a portable computer. The detector itself consists of a 1x1x1 cm3 Cadmium Zinc Telluride (CZT) crystal, and has a very small size and weight of around 60 grams. CZT has semiconductor properties and boasts a resolution of around 1.8 % at 661.6 keV. The detector has around 1 % of the sensitivity of a typical 25 % p-type HPGe detector. During the measurements, the detector was placed on an extendable rod protruding out from a tripod at 100 cm height above the ground surface. Spectra were acquired with Kromek's Multispect software until a satisfactory number of counts had been accumulated in the photopeak(s) of interest.

The second detector system was an Inspector 1000 MCA system from Canberra Industries (Belgium) coupled to a 1”x1” NaI probe. While the resolution of this type of detector (around 7 % at 662 keV) is inferior to the CZT detector, the sensitivity and robustness meant that it was a natural choice for a secondary system. Measurements were carried out with the detector placed on a tripod at 100 cm height, and spectra were accrued directly using the built-in software of the Inspector 1000.

Figure 5. *Detector systems used by the NRPA during GAMFAC exercise. Left: The CZT detector setup at Site 2 (red circle), together with the dose rate meter (hanging from the tripod). Right: NaI detector setup at Site 1.*

Both detector systems were calibrated before the exercise using methods described in Beck et al (1972) and elsewhere, taking point source measurements at normal incidence as well as at different angles and integrating over the polar angle. A picture of the typical NRPA

calibration setup can be seen in Figure 6. Further details of the detector calibration procedures are available in a previously published report (Mauring et al, 2014).

In addition to the spectrometric systems, ambient dose rates were measured with 6150AD 6/H dose rate meter manufactured by Automess GmbH (Germany) which had been calibrated at the NRPA's secondary standard dosimetry laboratory. The instrument was set to integrate the

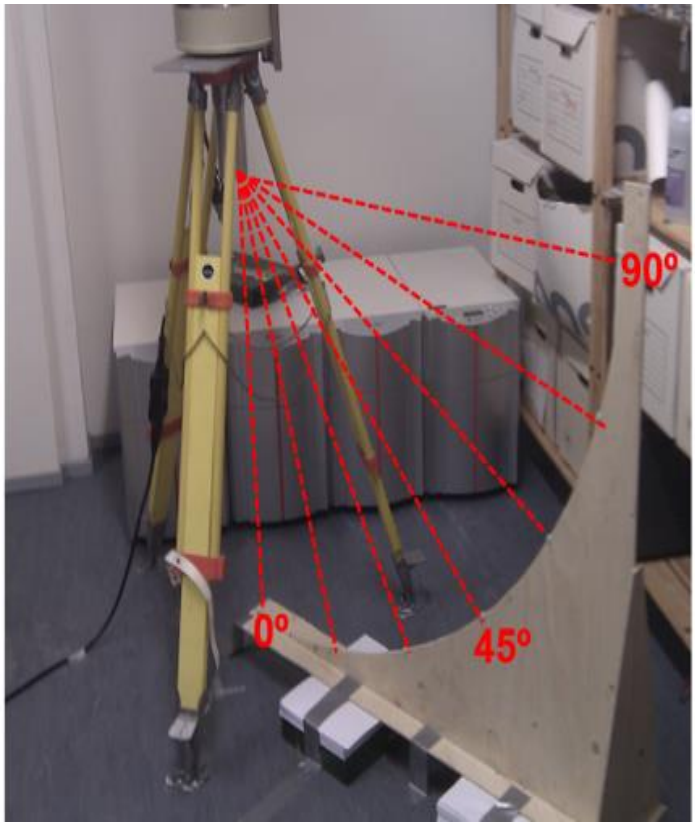

Figure 6. *Typical in situ detector calibration setup at the NRPA.*

dose over a period of approximately 10 minutes at each measurement location in order for the final result to be as accurate and precise as possible.

At each of the predefined sites, 3 - 4 in situ gamma spectrometric measurements of ^{137}Cs in the ground were performed with both CZT and NaI detector systems, as well as integrated dose rate measurements with the Automess. An average of the measurements was used in all subsequent calculations. In order to accurately compute the activity concentrations, assumptions must be made about the activity's distribution with depth. During the GAMFAC exercise, depth distributions and soil densities were estimated based on previous

characterizations performed by the laboratory of the Polessie State Radiation-Ecological Reserve (PSRER). Two different types of distribution models were used depending on the site characteristics: A slab model and an exponential model (Figure 7).

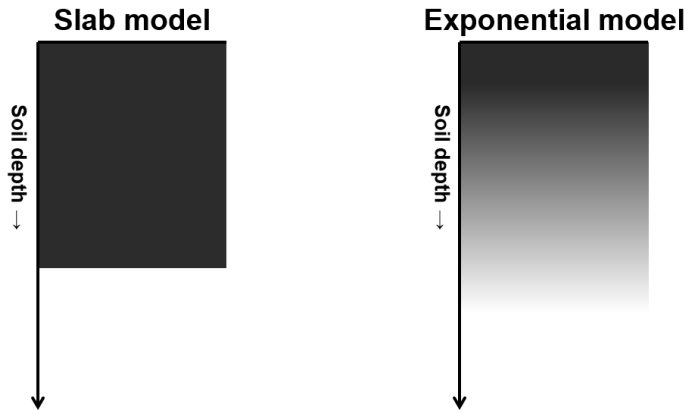

Figure 7. *Qualitative representation of the two types of depth distribution models used for activity estimations.*

With the slab model, the activity is assumed homogeneously distributed in the top layer of the soil, with the model parameters being the slab thickness and the physical density of the soil. The activity concentration can be expressed mathematically as a function of depth by:

$$A(z) = \begin{cases} A_0 & \text{for } 0 \leq z \leq a \\ 0 & \text{for } z > a \end{cases}$$

where A(z) is the activity at depth z, A_0 is the surface activity and a is the slab thickness.

The exponential model assumes that the activity is greatest at the soil surface and decreases exponentially with depth. This model is defined through a parameter commonly termed relaxation mass per unit area, which depends upon the relaxation length (equivalent to the soil depth at which 63 % of the activity is contained above) and the physical density of the soil. Mathematically, the exponential model is expressed as a function of soil depth by:

$$A(z) = A_0 \cdot \exp\left(-{}^{z}/_{\ell}\right)$$

where ℓ is the relaxation length per unit area. The parameter ℓ is used throughout the following sections on model assumptions and activity calculation results. The slab model for activity depth distribution is useful in cases where measurements are carried out on cultivated land and for soil types that are very penetrable with regards to contamination. The exponential distribution model is generally used for conventional soil types with radionuclides coming from older depositions. The in-house developed software tool InSiCal (Figure 8) was used to carry out all activity calculations. InSiCal is basically an advanced calculator that was developed to facilitate activity calculation in *in situ* gamma spectrometric measurements. It gives the user the possibility to vary all relevant parameters of the source model and measurement, and generates the various calibration factors used in this type of measurement scenario.

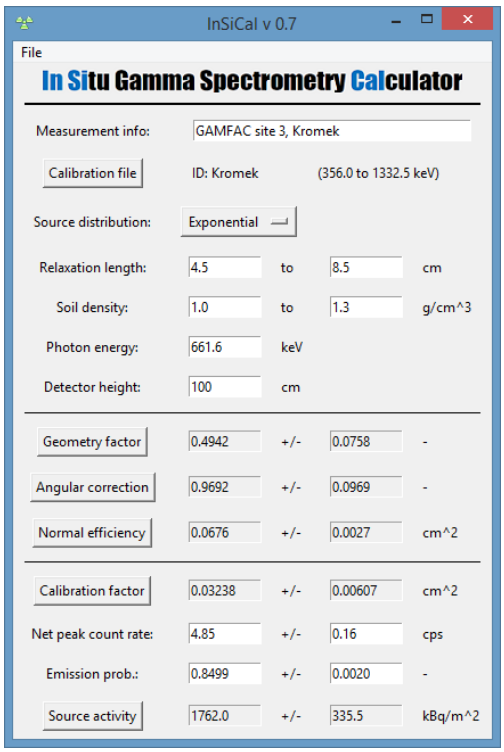

Figure 8. *Screenshot of the main window of the InSiCal tool.*

A detector specific calibration file can be input to calculate activity concentration directly. By taking into consideration the variation and uncertainty in the different input parameters, uncertainty computations are carried out automatically according to the latest ISO Guide 18589-7 (ISO, 2013). InSiCal also has the option of generating a measurement report file in simple text format so that calculations may be reproduced. During the actual *in situ* measurements preliminary results were calculated directly based on initial assumptions,

giving an approximate indication of the activity levels on the site. “Final” results were obtained within the same day. During post processing after the exercise, results for two of the sites (Site 3 and 4) were recalculated and adjusted for a deeper depth distribution than what was originally estimated. This was based on closer inspection of the soil core measurements.

3.1.2 Swedish Defence Research Agency, Sweden

For the GAMFAC activity the Swedish particpants chose a high resolution detector for *in situ* measurements to obtain an idea of what was possible to identify if there was a mix of nuclides present at the sites for the measurements. Since the supply of liquid nitrogen was a matter of uncertainty, the detector would also be preferably electrically cooled. The instrument chosen was an Ortec Detective EX High Purity Germanium detector. The Detective EX is a portable detector with an internal battery that gives an operating time of approx. three hours when fully charged. The detector is cooled with a Stirling Cooler which makes liquid nitrogen obsolete. The instrument has an internal processor so it can work without the support of a PC.

Figure 9. *The Ortec Detective EX High Purity Germanium detector employed by the Swedish team.*

If connected to a PC the touch screen is bypassed and the instrument is controlled with the computer.

The dimensions of the crystal of the detector as stated from the supplier:

- Detector crystal diameter: 50 mm
- Detector crystal length: 30 mm
- The efficiency relative a 3 × 3 inches NaI detector: 12 %
- Weight: 12 kg

The Detective EX is somewhat ruggedized so it is not as fragile as a lab instrument, which makes it convenient for field measurements. It has a handle to carry it and also a shoulder strap. The drawback with the electrical cooling system is that the instrument needs external power to turn the cooler on. This means that if it is run on battery only, the cooler needs to be maintained which limits the time of use to approx. three hours from the time it is unplugged from the charger. There is an option of using an external battery belt, which extends the time of operation. When connected to a computer with Ortec MCA emulation software installed the Detective EX will function as an HPGe spectrometer/Digital MCA. As the instrument is mainly used in laboratory settings, the GAMFAC project was a good opportunity to test the equipment in field. The setup for the measurements was that the detector was placed on a tripod with the crystal in a 90 degree angle to the ground and the center of the crystal at 1 m above the ground. The measurement time depended on the dose rate at the sites. Measurement times were long enough to ensure at least 1000 counts in the full-energy peak. All spectra were evaluated using Ortec GammaVision. For the dose rate measurements we used two different instruments. The Detective EX calculates the ambient dose rate equivalent from the gamma spectrum.

A Polimaster 1703 M, which is a small personal radiation detector, was also employed. It consists of a CsI crystal. It gives the personal dose rate equivalent as well as accumulated personal dose equivalent.

The Detective EX was automatically energy calibrated with an external ^{137}Cs source. The efficiency of the detector for the 661.6 keV energy was theoretically calculated with the equation

$$a_{esa} = \dot{N}_{in\,situ} \frac{\frac{a}{N_F}}{\frac{N_F}{N_0}}$$

where:

a_{esa} = Equivalent surface activity

$\dot{N}_{in\,situ}$ = Net peak area count rate

$\frac{a}{N_F}$ = Calibration coefficient

κ = Efficiency scaling factor

$\frac{N_F}{N_0}$ = Angular efficiency correction coefficient

The equation, factor and coefficients was obtained from Finck R.R (1992) except angular efficiency correction coefficient which was obtained from Helfer and Miller (1988). The calculation gave an efficiency for equivalent surface activity of 3.6×10^{-4} cps/Bq for ^{137}Cs (661.6 keV peak) for the Detective EX detector.

The efficiency of the detector was also semi calibrated for the 662 keV energy line by comparing the Detective EX with a 125 % HPGe detector with known efficiency for ^{137}Cs. The comparison was performed at a site with a known uniform distribution of ^{137}Cs activity. Both detectors were placed in the same spot and *in situ* measurements were performed. Afterwards, the net area of the photo peak for 662 keV was determined and the cps/Bq of ^{137}Cs was calculated. The difference between the Detective EX and the 125 % detector gave a factor that was used for ^{137}Cs calculations with the Detective EX. The efficiency for equivalent surface activity was calculated to 3.4×10^{-4} cps/Bq for ^{137}Cs.

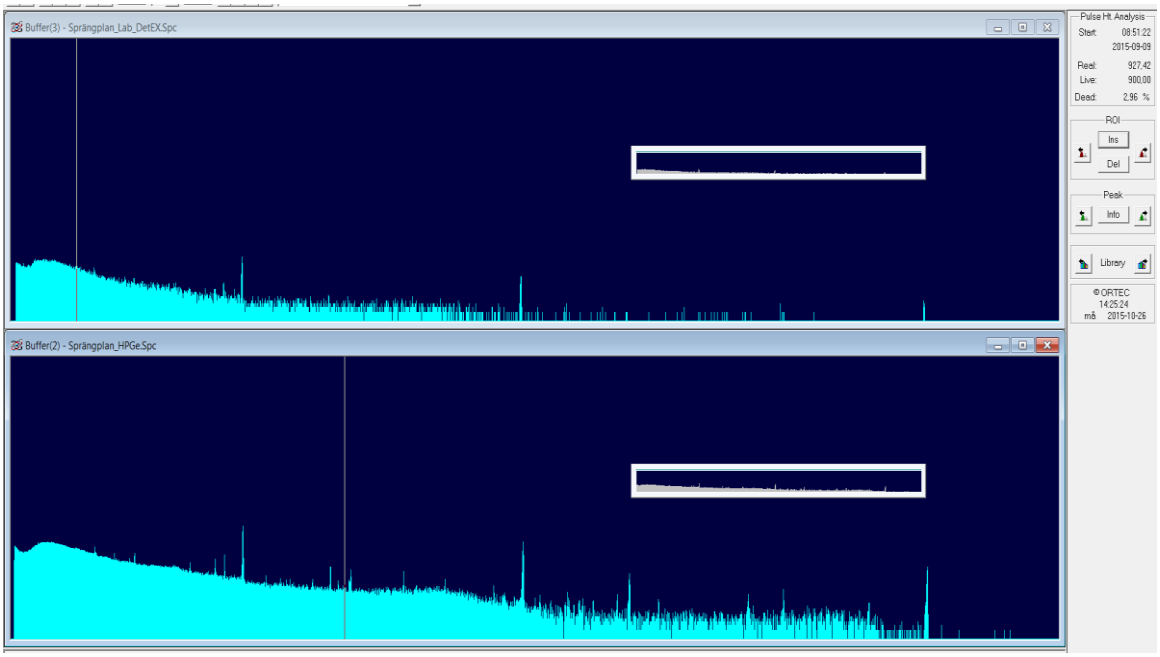

Figure 10. *Example spectra in Ortec GammaVision shows field measurements with the Detective EX (upper) and a 125 % HPGe detector (lower).*

The approach of the Swedish team was to use four different models with assumptions of soil density and distribution depths to evaluate the models since this information is not always available. Therefore, the information from soil samples/laboratory measurements was not used during measurements.

For the calculations of the ^{137}Cs activity at the measurement sites, four different models were used. The two first models were used at each site and then a third model was applied depending on the information to hand regarding the site distribution.

1. Equivalent surface activity – the activity per unit area on an infinite, plane surface.
2. Emergency preparedness model – the activity uniformly distributed in the 2 cm top layer of the soil, density = 0.5 g/cm3.
3. Uniform distribution – the activity uniformly distributed down to 20 cm of the soil layer, density = 1.6 g/cm3.
4. Exponential distribution – the activity exponentially distributed down to 10 cm of the soil layer, density = 1.6 g/cm3.

3.1.3. Danish Emergency Management Agency, Denmark

The Danish Emergency Management Agency (DEMA) used a Canberra Falcon electrically cooled Ge- detector to carry out in-situ measurement in the field (Figure 11). The Falcon has an extended range n-type detector with a relative efficiency of 20 %. The resolution is approximately 1.8 keV FWHM for 1332 keV. The instrument has a cooling time of approximately 4 hours and can be operated on battery power for at least 3 hours. Thus for a whole day of field work operation, the instrument needs to be plugged into external power between measurement series. This was done either by stopping at buildings with 220V between sites or by using a 400W 12V/22V converter which received power from the bus provided from Polessie State Reserve.

The Falcon runs Canberra Genie-2000 gammaspectrometry software, and was operated remotely by wifi from a ruggedized tablet computer. For data analyses, Canberra Geometry Composer and ISOCS (In Situ Object Counting System) sourceless calibration software were used. This way it was possible to calculate surface concentrations (Bq/m^2) that can be compared directly to the measurements done on samples by Polessie State Reserve.

Energy calibration of the Falcon Ge-detector is regularly done using ^{152}Eu, ^{137}Cs, ^{60}Co and ^{241}Am sources. Efficiency calibration is entirely done using the detector characterization data,

Figure 11. *The Canberra Falcon Ge-detector mounted on a tripod at Site 1.*

which is delivered with the instrument and the sourceless calibrations software mentioned above. The instrument had not been calibrated specifically for in-situ measurements and DEMA had prior to the field work in Belarus in September 2015 no procedure for doing in-situ measurement and calculating surface contaminations.

The data obtained at the six sites described in chapter 3.2 are shown in Table 1. At least 5 measurements were done at each site (with the exception of Site 6) at the location of the poles that were already mounted at the sites. The data was measured between 0.75 m and 1 m above ground. Most measurement were performed with the detector mounted on a tripod (Figure 11), but some was done where the detector was handheld. The measurements shown in Table 1 were acquired with a counting time between 120 and 600 s, except at Site 6, where the counting time was 914 s (Table 1). Cs-137 was the only man made radionuclide identified at any of the 6 sites. Counting statistics for the full energy peak of ^{137}Cs at 662 keV was normally better than 1% at 1 sigma. However, for Site 6, which had the lowest dose rate, counting statistics was 2.9 %. Dead time correction was always less than 9 % and FWHM was

between 1.41 and 1.7 As mentioned above data was acquired with Genie-2000 (see Figure 12). Later, Genie-2000 was used to calculate the activity of ^{137}Cs expressed as kBq/m^2.

Calculation of the efficiency of ^{137}Cs (662 keV) was done using ISOCS. For this study, a disk geometry with a diameter of 200 m and a thickness of 20 cm was constructed (Figure 12). Two different disk shaped distribution models was used. The first is a slab model where the activity is evenly distributed. The other is a five layer model where the activity decreased by 33 % with each layer. For both models, the detector was situated at the center of the disk and at a distance of 0.85 m. This geometry imitates a slab of soil with a density of 1.6 g/cm^3 under the detector when it is mounted on a tripod 0.85 m above ground. The diameter of the disk, which signifies the maximum horizontal detection distance of the detector, was determined by increasing the diameter of the disk model until activity pr. area was constant (Figure 12). It is seen from Figure 12 that the activity of a given disk shape sample increases until a certain level (> 200 m). Beyond this distance from the detector the detection of photons with an energy of 662 keV is no longer significant.

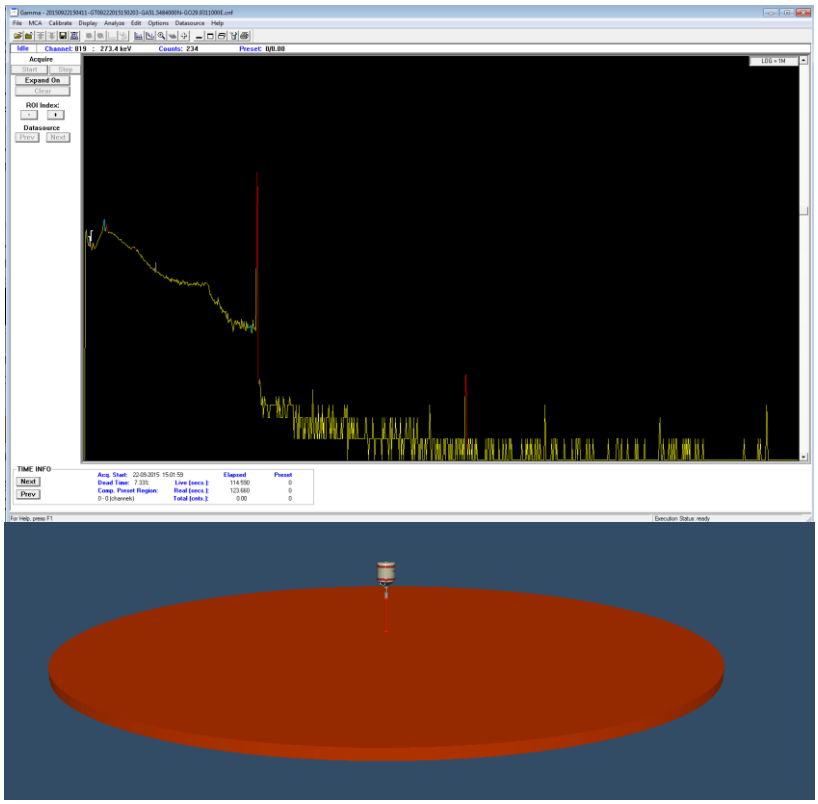

Figure 12. *Typical spectra from Genie-2000 (top). Note the ^{137}Cs full energy peak at 662 keV. Picture from Canberra Geometry Composer (bottom). The geometry used is a disc shaped sample with a diameter of 200 m and a thickness of 20 cm.*

Site	Dato	Spektrum ID	real time	Dead time (%)	Cs-137 (662 keV) counts	+/- %	FWHM (keV)	cps	Doserate (mikroSv/h)	kBq/m2 (Polessie data)	Distribution model	Soil type	Soil density g/m3	kBq/m2 (DEMA)	Deviation (DEMA-Polessie)
1,1	22-09-2015	125716	128,01	8,24	36664	0,53	1,641	312,14	2,28	2414	0-20 cm/exp	Sosoddy podzolic soilil	1,62	2088	14%
1,2	22-09-2015	130007	126,55	8,36	36623	0,53	1,674	315,80		2414	0-20 cm/exp	Sosoddy podzolic soilil	1,62	2113	12%
1,3	22-09-2015	130325	125,69	8,81	41224	0,5	1,642	359,66		2414	0-20 cm/exp	Sosoddy podzolic soilil	1,62	2406	0%
1,4	22-09-2015	130733	130,55	8,49	39948	0,51	1,647	334,38		2414	0-20 cm/exp	Sosoddy podzolic soilil	1,62	2237	7%
1,5	22-09-2015	131055	124,19	8,25	36102	0,53	1,661	316,82		2414	0-20 cm/exp	Sosoddy podzolic soilil	1,62	2119	12%
1,5	22-09-2015	131628	305,95	8,15	84424	0,35	1,638	300,41		2414	0-20 cm/exp	Sosoddy podzolic soilil	1,62	2010	17%
1,5	22-09-2015	132231	303,95	8,96	110210	0,3	1,618	398,26		2414	0-20 cm/exp	Sosoddy podzolic soilil	1,62	2664	-10%
2,1	23-09-2015	120701	308,73	1,65	5532	1,36	1,634	18,22	0,25	215	0-20 cm/slab	Sand	1,77	299	-39%
2,2	23-09-2015	121244	307,44	1,47	3669	1,66	1,748	12,11		215	0-20 cm/slab	Sand	1,77	199	7%
2,3	23-09-2015	121827	306,35	1,51	4587	1,49	1,736	15,20		215	0-20 cm/slab	Sand	1,77	250	-16%
2,4	23-09-2015	122941	306,84	1,65	4982	1,43	1,621	16,51		215	0-20 cm/slab	Sand	1,77	271	-26%
2,5	23-09-2015	122411	305,61	1,69	5398	1,37	1,655	17,97		215	0-20 cm/slab	Sand	1,77	295	-37%
3,1	22-09-2015	145115	125,96	6,79	25344	0,63	1,638	215,86	1,76	1672	0-20 cm/exp	Peat	1,15	1444	14%
3,2	22-09-2015	145751	128,88	7,30	31838	0,57	1,583	266,49		1672	0-20 cm/exp	Peat	1,15	1783	-7%
3,3	22-09-2015	150654	126,38	7,26	30794	0,54	1,58	262,75		1672	0-20 cm/exp	Peat	1,15	1758	-5%
3,4	22-09-2015	150105	125,6	7,46	31838	0,57	1,583	273,92		1672	0-20 cm/exp	Peat	1,15	1883	-13%
3,5	22-09-2015	150411	123,66	7,33	32405	0,56	1,625	282,79		1672	0-20 cm/exp	Peat	1,15	1892	-13%
4,1	23-09-2015	105157	638,92	3,15	66204	0,39	1,625	106,99	0,94	1178	0-20 cm/exp	River bed	1,23	716	39%
4,2	23-09-2015	*105831*	311,05	6,42	93903	0,33	1,623	322,59		1178	0-20 cm/exp	River bed	1,23	2158	-83%
4,3	23-09-2015	110501	323,89	4,50	61858	0,41	1,632	199,99		1178	0-20 cm/exp	River bed	1,23	1338	-14%
4,4	23-09-2015	111120	306,22	3,15	29404	0,59	1,621	99,15		1178	0-20 cm/exp	River bed	1,23	663	44%
4,5	23-09-2015	111715	306,02	3,47	35632	0,59	1,672	120,63		1178	0-20 cm/exp	River bed	1,23	807	32%
5,1	21-09-2015	132454	317,22	1,10	7079	1,2	1,648	22,56	0,28	644	0-20 cm/slap	Ploved field	1,55	371	42%
5,1	21-09-2015	133055	306,27	1,14	7738	1,15	1,595	25,56		644	0-20 cm/slap	Ploved field	1,55	420	35%
5,2	21-09-2015	140519	304,55	1,12	6885	1,22	1,635	22,86		644	0-20 cm/slap	Ploved field	1,55	375	42%
5,2	21-09-2015	141107	304,19	1,14	7318	1,18	1,639	24,34		644	0-20 cm/slap	Ploved field	1,55	400	38%
5,5	21-09-2015	141853	305,59	1,27	8623	1,09	1,62	28,58		644	0-20 cm/slap	Ploved field	1,55	469	27%
5,4	21-09-2015	142542	331,78	1,22	8490	1,1	1,537	25,90		644	0-20 cm/slap	Ploved field	1,55	425	34%
5,3	21-09-2015	143333	309,36	1,25	8261	1,11	1,622	27,04		644	0-20 cm/slap	Ploved field	1,55	444	31%
5,1	21-09-2015	144609	618,84	1,15	15011	0,84	1,599	24,54		644	0-20 cm/slap	Ploved field	1,55	403	37%
	21-09-2015	145532	378,2	1,24	10082	1,01	1,583	26,99		644	0-20 cm/slap	Ploved field	1,55	443	31%
6	24-09-2015	83234	914,78	0,14	1310	2,87	1,407	1,43	0,14	13	0-20 cm/slab	Stadion/grass	-	24	-81%

Table 1. *In situ measurement data and calculations performed by Danish Emergency Management Agency (DEMA).*

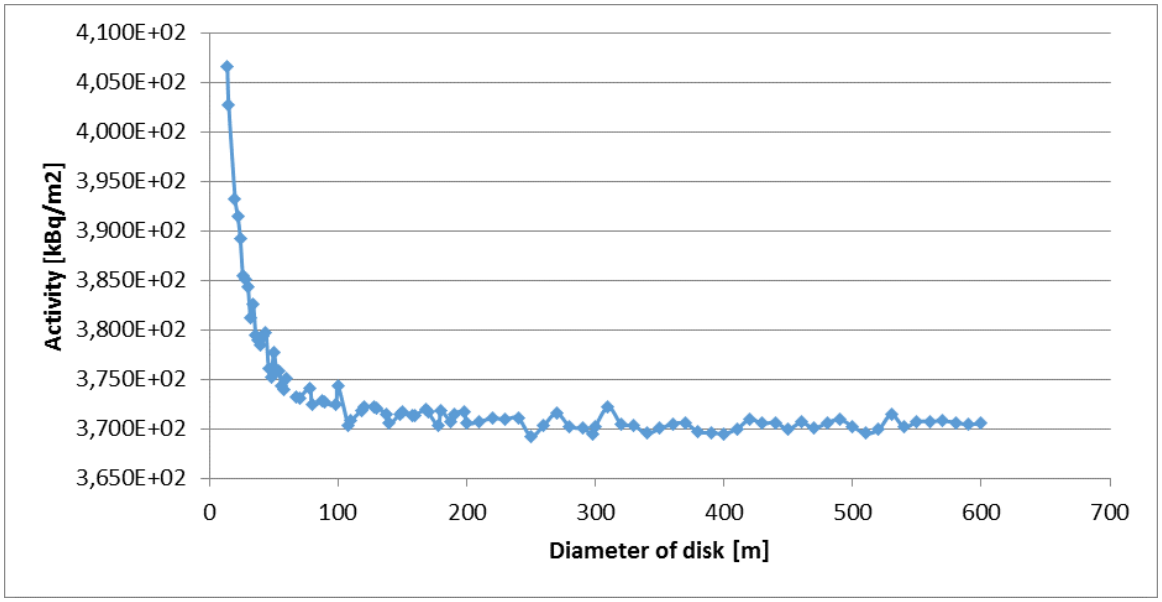

Figure 13. *Activity of ^{137}Cs in kBq/m^2 of a disk shape sample with variable diameter and the detector located in the center of the disk (0.85 m above).*

3.1.4. Stirling University, Scotland.

The Environmental Radioactivity Lab (ERL) based at the University of Stirling specialises in environmental radioactivity monitoring and regularly undertakes habit surveys, dose assessments and soil, vegetation and water sampling. A large part of the work that ERL conducts also involves a wide range of in situ measurements, which it has been developing for the past 20 years. Within the Belarussian exclusion zone, ERL deployed fully calibrated equipment to fulfil 3 aims:

i. Estimate the overall trend in activity and burial distribution of ^{137}Cs within the soil column at the 5 designated site.
ii. Estimate the dose rate at individual sites.
iii. Map local heterogeneity in depth and activity distribution of ^{137}Cs across individual sites to potentially reveal spatial patterns and any interesting radiological features.

To address (i), conventional static in situ measurements were made using mid-energy resolution scintillation detectors, deployed at 1 m above the ground, over a 300 second period (Figure 1). This provided a clear energy spectrum to develop source estimates from.

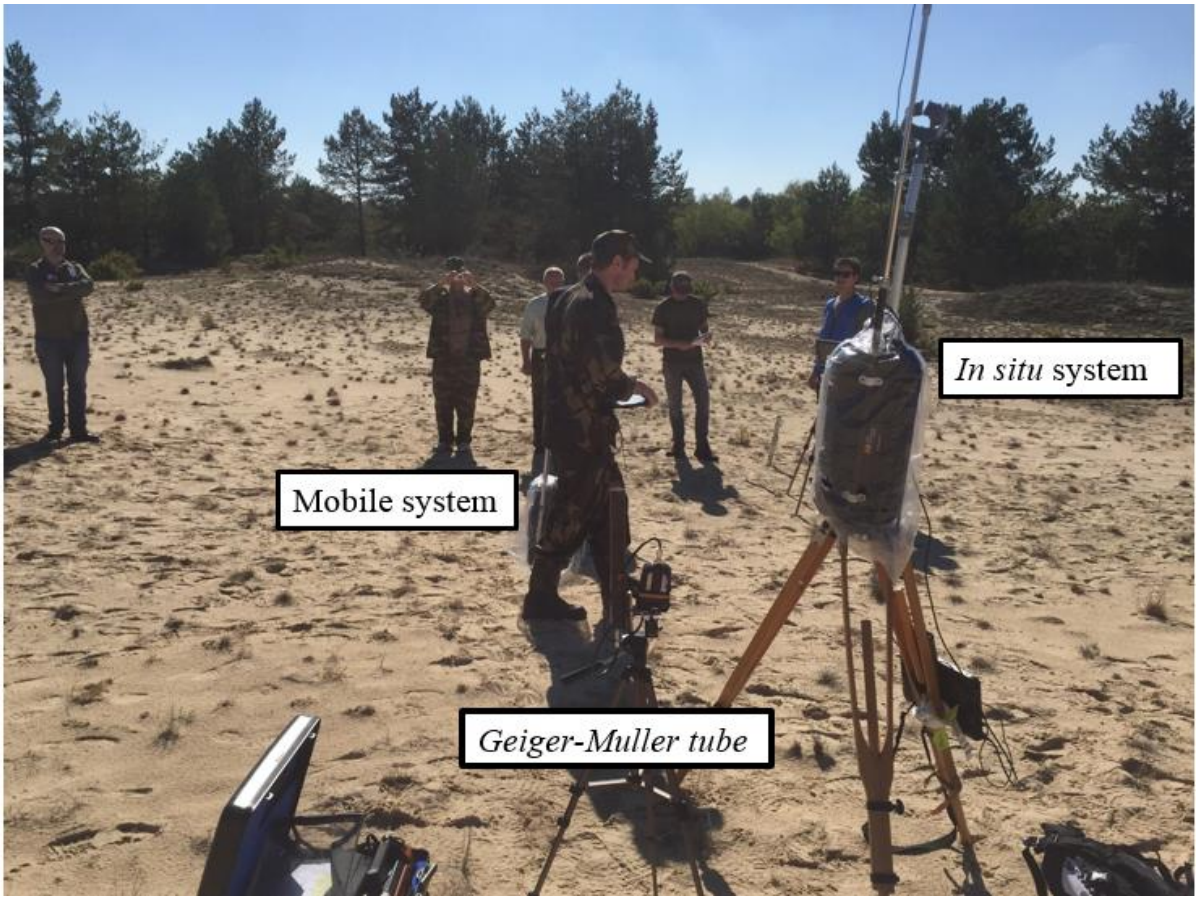

Figure 14. *Photograph demonstrating the 3 detector setup used by ERL including in situ, mobile system and Geiger-Muller tube.*

Crucially, the spectral processing method employed, which was based upon the relationship between full energy and forward-scattered photons (Zombori et al., 1992, Tyler, 2008), did not require any prior knowledge of activity distribution derived from soil cores. The theory of the method assumes that with greater source burial depth there will be a larger number of forward-scattered photons, thus losing a small amount of energy, and accumulating between the full energy peak and Compton edge in the detector's spectrum (Figure 15). This relationship was modelled using a straightfoward regression model.

Effective dose (ii) was estimated using a Geiger-Müller tube (Figure 14) and ICRP conversion factors (1987), following ERL's ISO17025 accredited methodology. The Geiger-Müller tube was left to count for 600 seconds to attain acceptable uncertainty. To assess the potential heterogeneity at individual sites (ii), a minimum of 1000 of 1 second count measurements, taken approximately 0.1 m above the ground, were recorded alongside DGPS

coordinates using portable systems built by ERL named Stirling Mobile Gamma-ray Spectrometry System (SMoGSS) (Figure 14). SMoGSS can be operated on scintillation detectors and the DGPS device (SSX blue) records to an accuracy of 0.6 m. The software provides real-time feedback of each energy spectrum, tracking of energy windows and alarms. At present, the alarms operated on SMoGSS are tailored towards hot particle detection. However these were disabled for work in the exclusion zone. A screenshot of SMoGSS can be found in Figure 16, including individual window time-series, rainbow diagram and raw spectral output.

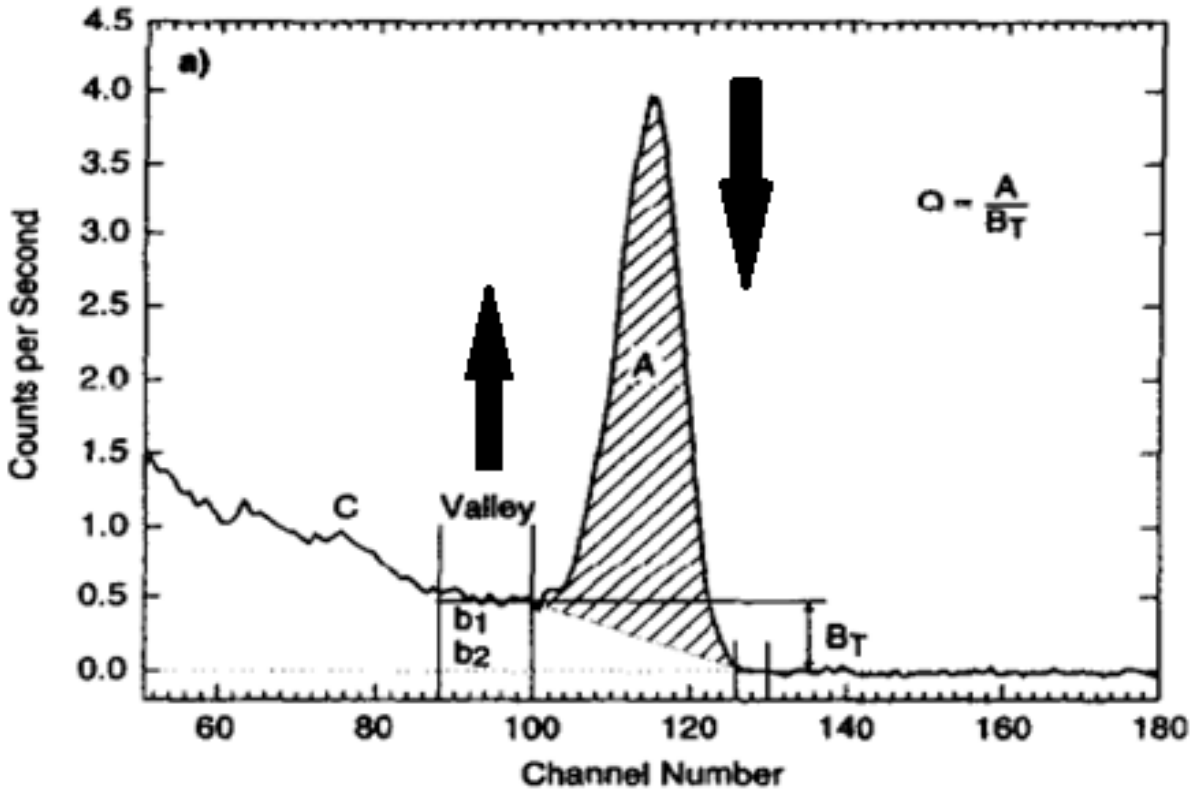

Figure 15. *Illustration of peak to valley ratio.*

Point data collected from SMoGSS was then interpolated to create a smoothed 3-dimensional raster with the variables effective depth (α) and activity (kBq m^{-2}). Effective depth of a source follows adheres to an exponential model where values controlling the shaping parameter range between 0 and 1. Values closer to 0 are homogeneous in the z plane (similar to a slab model) and values closer to 1 have more contamination associated with surface sediments (Beck et al., 1972).

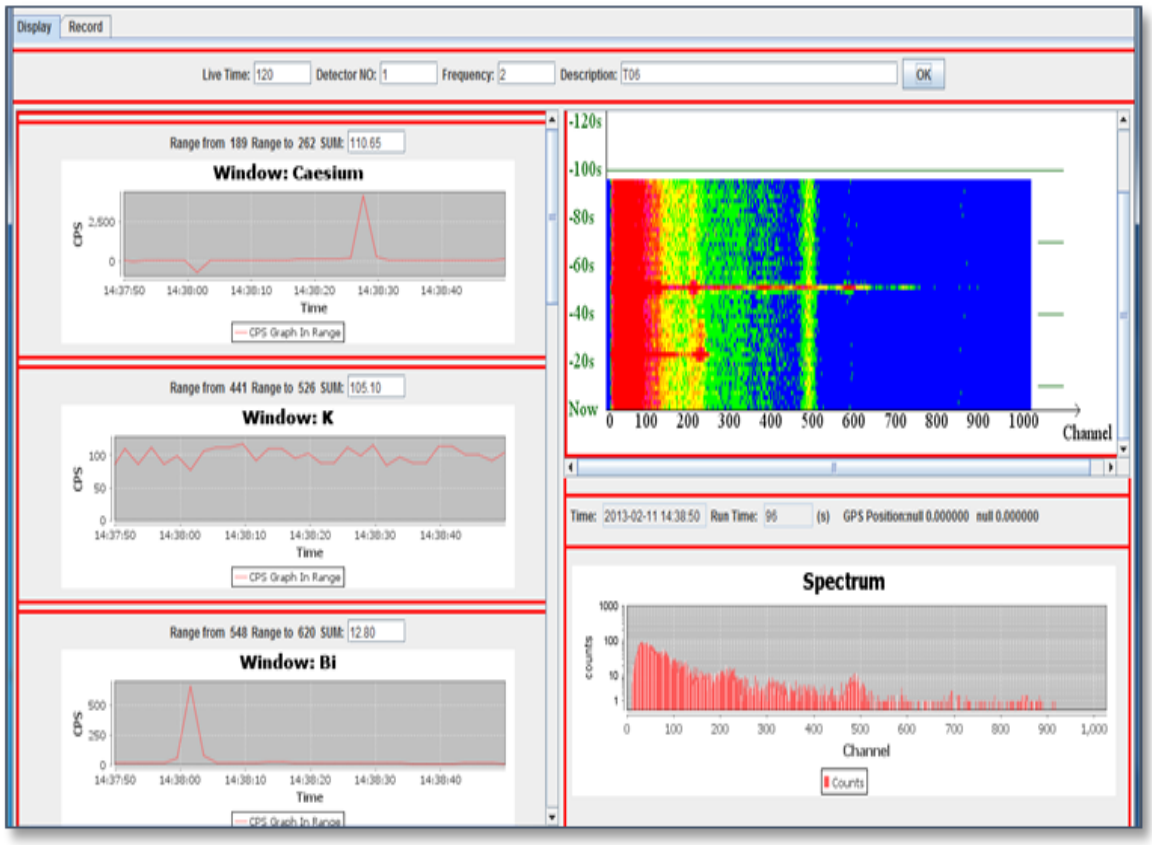

Figure 16. *Screenshot of SMoGSS including rainbow diagram and raw spectral output.*

Monte Carlo simulations were used to calibrate spectral data. Whereby the depth and activity of the source was controlled to generate spectral responses. Furthermore, uncertainties associated with soil density, background contributions and counting statistics were also included in simulations. All Monte Carlo simulations were performed in Monte Carlo N-Particle eXtended (MCNPX) (Briesmeister, 1993). A visualisation of the modelling geometry can be observed in Figure 17. The first instrument, a 71 × 71 mm Sodium Iodide (NaI:Tl) scintillation detector, was purchased from Saint-Gobain crystals in 2007 (Figure 18). ERL has employed this detector in a number of applications, such as in situ baseline surveys around nuclear establishments, monitoring radio-caesium in the Ukrainian exclusion zone and beach monitoring for ^{226}Ra containing "hot" particles. NaI:Tl is used extensively in environmental monitoring for a number of reasons; predominantly because it is lightweight (~4kg), possesses acceptable energy resolution (~7% at 662 keV) and energy efficiency (~90% at 662 keV), can process individual pulses relatively fast (230 ns), is relatively cheap and has low power requirements (Knoll, 2010). ERL controls the detector's Multichannel

Analyser (Ortec's DigiBase) using Ortec's Maestro software (ORTEC, 2005), allowing a spectrum to be acquired over a set time period.

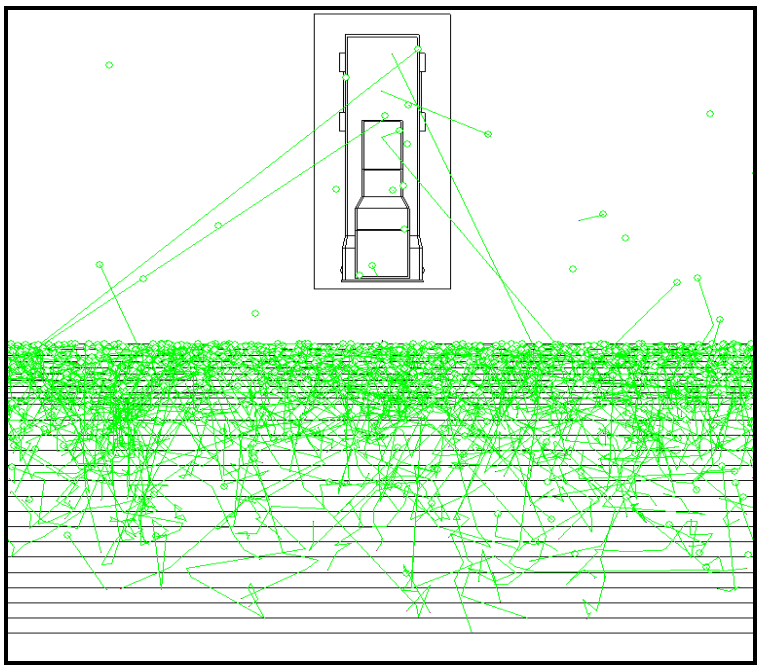

Figure 17. *Visualisation of Monte Carlo model used to calibrate detectors. Photon tracks are included.*

Figure 18. *71 × 71 mm Sodium Iodide detector*.

The second instrument, also a 71 × 71 mm scintillation detector, Lanthanum Bromide (LaBr:Ce), was purchased from Saint Gobain in 2012 by Nuvia UK. It was chosen for the same reasons as NaI:Tl, but has the added advantage of better energy resolution (~3.5%) (Figure 19), greater energy efficiency (~9% higher at 662 keV) and a much faster decay time (28 ns). However, LaBr:Ce bromide is known to be affected by intrinsic contamination owing to the naturally occurring radioelements ^{227}Ac and ^{138}La (Menge et al., 2007). This can lead to difficulties when trying to measure low activities in the environment, although at the count rate observed in the exclusion zone, this was not found to significantly influence results. Another considerable factor governing the choice of LaBr:Ce is that is an order of magnitude more expensive than a comparable NaI:Tl detector.

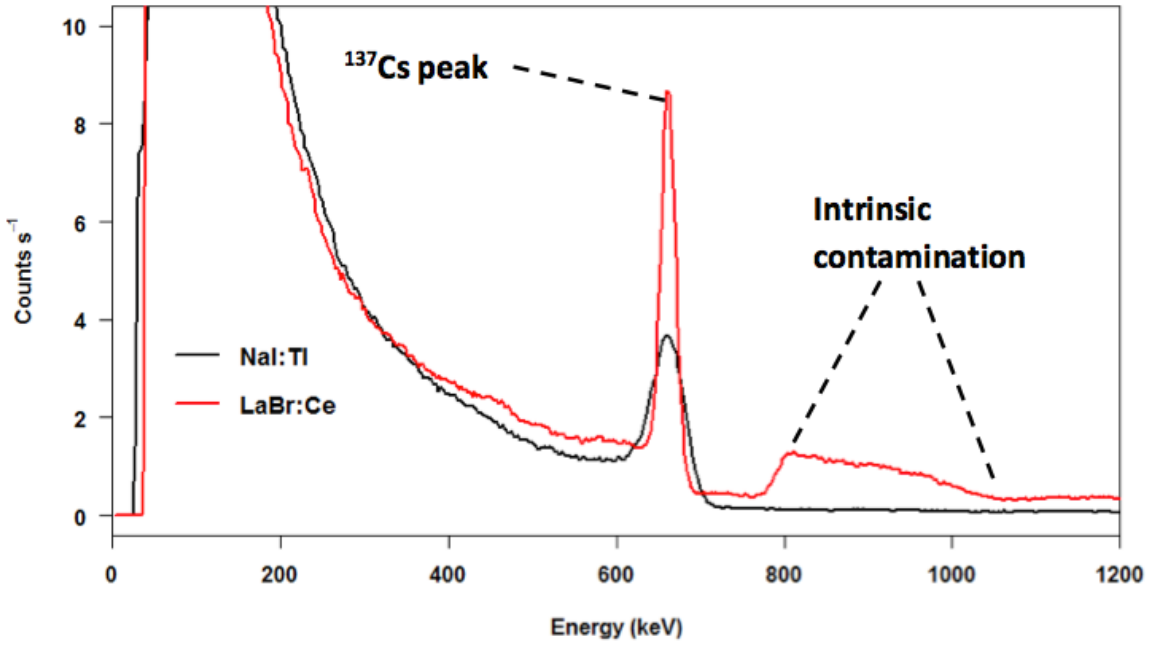

Figure 19. *Spectral responses of sodium iodide and lanthanum bromide exposed to a ^{137}Cs source. Intrinsic contamination is highlighted for lanthanum bromide.*

A third instrument, a Geiger-Müller tube, made by Thermo Radeye instruments was employed to estimate the dose at each site using ICRP conversion factors to convert to Effective dose. ERL has used this instrument to measure dose rates all over the United Kingdom and calibrated in the laboratory used a ^{137}Cs point source. It is also accredited under ISO17025.

3.1.5. Icelandic Radiation Protection Authority, Iceland

The Icelandic team used an OTREC LN2-cooled HPGe detector (GEM15P4-70-S type) with a measured relative efficiency of 18% at 1.33 MeV (see Figure 20). The crystal size was 49.8 mm x 50.2 mm so a relatively flat spatial response could be assumed. The MCA was an ORTEC digiDART.

Three kinds of handheld meters were used: two Thermo Fischer RadEye G-10 Gamma Survey Meters, a RADOS RDS-110 Multi-Purpose Survey meter and a SAIC Exploranium GR-135 ”The Identifier”. In general, they showed similar values for dose rates, which again were in good agreement with the already established values for each site. The GR-135 has a built-in isotope identification feature but ^{137}Cs was the only isotope that it could identify, and sometimes even this was not identified, possibly due to the complex radiation situation in the area.

LN2-cooled HPGe detectors have the advantage that they can easily be kept at an operational temperature for the duration of a multi-day mission without external power supply given the availability of LN2, and the cooling system is not prone to malfunction. Thus they can be used for continuous mobile monitoring and mapping of a survey area in addition to specific on-site measurements. The use of LN2 does, however, require careful planning due to transportation issues etc., related both to the transportation of LN2 and the detector system itself.

The HPGe detector was mounted on a tripod so that the center of the crystal was 1 m above the ground surface. Measurement times for each spectrum were from 7-15 minutes and one to four measurements were made at each site. Only one measurement from each site was used for calculating the ^{137}Cs activity. The HPGe detector was close to saturation in the most contaminated locations, most notably at sites 1 and 3. Dead time was between 3 and 21%, while dead time at the ”control” site (Site 6) was 0.55%. The net count rates for the ^{137}Cs peak ranged from 15 to 353 cps (1 cps at the ”control” site). This detector would be inapplicable near ground in the case of significant fresh fallout, e.g. including Iodine, in which case it could be used as part of an airborne measurement system or for measurements of samples in a controlled environment away from the contaminated area.

Figure 20. *The Icelandic team detector in two height configurations (left and top right) and while filling liquid nitrogen (bottom right).*

3.2 The Test Locations

Six locations were prepared in advance for the activities of GAMFAC by the staff of the reserve. Prior to the activity the general requirements for the GAMFAC test sites was communicated to the staff of the reserve. These requirements included the area of the sites, the nature of the land on which the sites were to be located, contamination levels, absence of trees, etc. The primary goal in establishing these requirements was that sites could be found on essentially flat terrain without overhanging trees or exposed geology such that confounding factors to the conducting of accurate in-situ measurements were not present. The sites were to represent a range of soil types present in the reserve and different levels and

depth distributions of contamination. The sites were to be relatively near roads to limit manual carrying of equipment and pre-activity characterisation of the sites should have been conducted in relation activity levels etc. This characterisation work was carried out in the summer of 2015 prior to the GAMFAC activity proper. One of the sites selected was a "control" site with no appreciable levels of contamination. The purpose of this site was to facilitate background measurements or to ensure that detectors and other equipment were not making false positive measurements for whatever reason. A second site was agricultural land with, it was assumed, a relatively even distribution of contamination due to agricultural ploughing that had been conducted there. The aim of this site was the provision of a site where the down column distribution was substantially different that at the other sites chosen and where models related to even distributions within the soil column could be tested. The other four sites varied, as dicussed previously, according to soil type, level of contamination present and the nature of the vertical distribution of the contamination within the soil column. More detailed descriptions of the sites, their characteristics and radionuclide inventories are provided in following sections. The selected sites were flat lands, being not less than about 50 m in diameter. In the center of each site a square area was marked with dimensions about 10×10 m. The gamma dose rate was measured using an AT6130 Radiation Monitor (produced by Scientific and Production Enterprise ATOMTEX, Belarus) in each corner of the square and in the center at a height of 1 m above the soil surface. At the same points the soil samples were taken. The geographic coordinates were registered using GPS. A standard cylindrical sampler of diameter 4 cm and capable of sampling to 20 cm depth was used to take the soil samples from the corners of the selected square area (10×10 m) and from its center. Each core, beginning from the deeper layers, was divided into the following layers: 0-3 cm, 3-6 cm, 6-10 cm, 10-15 cm, 15-20 cm. All layers of the same depth from the five cores were combined and homogenized providing complete filling of the measurement vessel for gamma-spectrometry. In total 25 samples were taken from Sites 1 – 5. In case of Site 6 (background check) there was no dividing based on depth – five cores 0-20 cm were combined and homogenized. The preparation of soil samples for the radioanalytical measurements included air drying and homogenization by thoroughly mixing and screening through a 2 mm sieve. After weighing of the subsample, it was transferred to the analytical vessel adopted for counting. A gamma-spectrometer from Canberra was used for the instrumental determination of both ^{137}Cs and ^{241}Am. The spectrometer utilised a Be5030 detector of high purity germanium with a carbon window and a relative efficiency of 50 % connected to a DSA 1000 multichannel analyzer. The volume of analytical sample was equal to 100 cm^3. Duration of measurement varied from

6000 to 80000 sec. Statistical uncertainties of the square of the complete absorption peak of ^{241}Am and ^{137}Cs were less than 10 and 5 %, accordingly. The instrumental determination of ^{90}Sr was carried out with help of an AT1315 gamma-beta-radiation spectrometer ("Atomtex", Belarus). In this instrument, a detection block based on a NaI(Tl) scintillation crystal of 63mm height and diameter was used to register gamma-radiation. An organic scintillator of polystyrene of 9 mm height and 128 mm diameter was used to register beta-radiation. The software of the gamma-beta-spectrometer allows for calculating the activity of radionuclides in the sample by computer spectra processing using a maximum likelihood method. The data for gamma- and beta-spectrometric measurements are analyzed and processed simultaneously. The method assumes that the radionuclide composition of the sample is known and the sample doesn't contain other artificial radionuclides apart from ^{137}Cs and ^{90}Sr. In spite of the high low limit of determination of ^{90}Sr (20 Bq/kg), this device is suitable for the intended use and is widely applied in the laboratory for the analysis of environmental samples contaminated by Chernobyl fallout. The measurment time was equal to 1800 sec.

Site 1.

Site 1, N 51º33′07,9″ E 029º55′26,1″ (Figure 21), was a soddy podzolic soil exhibiting dose rates in the range 2.21 to 2.50 μSv/h at 1 m height. Site 1 had the highest ^{137}Cs contamination of all the GAMFAC sites with significant levels of ^{241}Am and ^{90}Sr present (Table 2.).

Layer	**Layer Mass g**	**^{137}Cs Bq/kg**	**Percentage of ^{137}Cs in each layer**	**^{90}Sr Bq/kg**	**Percentage of ^{90}Sr in each layer**	**^{241}Am Bq/kg**	**Percentage of ^{241}Am in each layer**
0-3 cm	193.6	41450+/-8290	66.1+/-13.2	1260+/-557	13.6+/-6.0	187+/-45	52.9+/-12.7
3-6 cm	227.6	15350+/-3070	28.8+/-5.8	900+/-310	11.5+/-3.9	109+/-26	36.2+/-8.6
6-10 cm	321.8	1360+/-270	3.6+/-0.7	1165+/-263	21.0+/-4.7	16.2+/-3.8	7.6+/-1.8
0-15 cm	431.2	314+/-72	1.1+/-0.3	1344+/-292	32.4+/-7.0	3.8+/-1,1	2.4+/-0.7
15-20 cm	453.8	92+/-27	0.3+/-0.1	850+/-193	21.6+/-4.9	1.4+/-0.5	0.9+/-0.3
Contamination Density kBq/m^2		2414		356		14	

Table 2. *Characteristics of contamination within the soils of Site 1. Soil bulk density at Site 1 – 1.62 g/cm^3.*

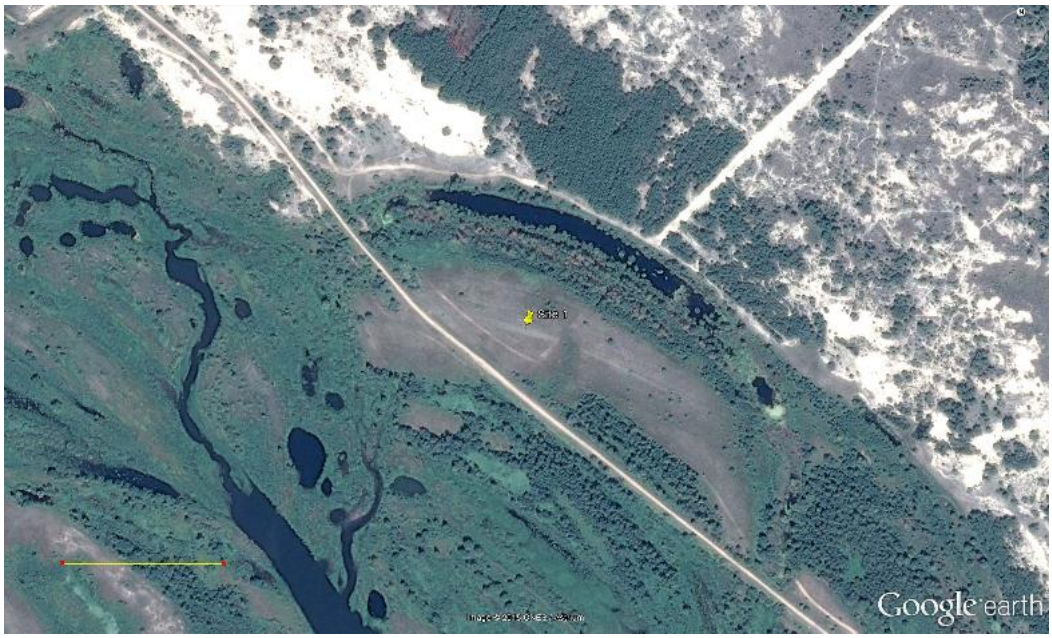

Figure 21. *Site 1 location from above and from ground level. Yellow line indicates 200 m scale.*

Site 2

Site 2, N 51º33′17,1″ E 029º55′12,1″, was a primarily sandy soil exhibiting dose rates in the range 0.29 to 0.35 µSv/h at 1 m height (Figure 22). Site 2 had ^{137}Cs contamination amongst the lowest of all the GAMFAC sites with insignificant amounts of ^{90}Sr present and low levels of ^{241}Am (Table 3).

Figure 22. *Site 2 location from above and from ground level. Yellow line indicates 200 m scale.*

Layer	Layer Mass g	^{137}Cs Bq/kg	Percentage of ^{137}Cs in each layer	^{90}Sr Bq/kg	Percentage of ^{90}Sr in each layer	^{241}Am Bq/kg	Percentage of ^{241}Am in each layer
0-3 cm	295.8	876+/-175	24.0+/-4.8			1.3+/-0.5	20.4+/-7.8
3-6 cm	256.8	814+/-163	19.4+/-3.9			1.5+/-0.7	20.4+/-9.5
6-10 cm	352.0	693+/-139	22.6+/-4.5			1.3+/-0.5	24.2+/-9.3
0-15 cm	443.6	813+/-163	33.4+/-6.7			1.2+/-0.6	28.2+/-14.1
15-20 cm	428.6	16+/-8	0.6+/-0.3			0.3+/-0.2	6.8+/-4.5
Contamination Density kBq/m^2		215				0.38	

Table 3. *Characteristics of contamination within the soils of Site 2. Soil bulk density at Site 2 – 1.77 g/cm^3.*

Site 3

Site 3, N 51º32′54,7″ E 029º55′52,2″ (Figure 23), was a primarily organic peat soil exhibiting dose rates in the range 1.55 to 1.73 µSv/h at 1 m height. Site 3 had the second highest ^{137}Cs contamination amongst all the GAMAC sites with appreciable amounts of ^{90}Sr present and levels of ^{241}Am.

Layer	Layer Mass g	^{137}Cs Bq/kg	Percentage of ^{137}Cs in each layer	^{90}Sr Bq/kg	Percentage of ^{90}Sr in each layer	^{241}Am Bq/kg	Percentage of ^{241}Am in each layer
0-3 cm	97.4	33380+/-6675	38.7+/-7.7	3740+/-886	18.5+/-4.4	210+/-50	37.7+/-9
3-6 cm	158.2	16000+/-3200	30.1+/-6.0	2775+/-604	22.3+/-4.9	113+/-27	32.9+/-7.9
6-10 cm	246.4	5910+/-1180	17.3+/-3.5	2590+/-543	32.5+/-6.8	40.9+/-10.3	18.6+/-4.7
0-15 cm	306.0	2740+/-550	10.0+/-2.0	1210+/-274	18.8+/-4.3	14.7+/-3.8	8.3+/-2.1
15-20 cm	347.0	947+/-189	3.9+/-0.8	446+/-107	7.9+/-1.9	3.9+/-1.1	2.5+/-0.7
Contamination Density kBq/m^2		1672		319		11	

Table 4. *Characteristics of contamination within the soils of Site 3. Soil bulk density at Site 3 – 1.15 g/cm^3.*

Figure 23. *Site 3 location from above and from ground level.*

Site 4

Site 4, N 51º31′45,2″ E 029º56′07,5″ (Figure 24), was a regularly flooded soil exhibiting dose rates in the range 0.52 to 0.89 µSv/h at 1 m height. Site 4 had the second highest ^{137}Cs contamination in excess of 1 MBq/m^2 with appreciable amounts of ^{90}Sr present and levels of ^{241}Am (Table 5).

Layer	**Layer Mass g**	**^{137}Cs Bq/kg**	**Percentage of ^{137}Cs in each layer**	**^{90}Sr Bq/kg**	**Percentage of ^{90}Sr in each layer**	**^{241}Am Bq/kg**	**Percentage of ^{241}Am in each layer**
0-3 cm	80,2	41810+/-8360	56.6+/-11.3	1018+/-299	8.3+/-2.5	1347+/-312	66.2+/-15.3
3-6 cm	151,5	8665+/-1733	22.2+/-4.4	1062+/-295	16.5+/-4.6	236+/-53	21.9+/-4.9
6-10 cm	258,6	3076+/-615	13.4+/-2.7	705+/-209	18.6+/-5.5	54.5+/-12.4	8.6+/-2.0
0-15 cm	373,8	940+/-189	5.9+/-1.2	774+/-178	29.6+/-6.8	12.4+/-2.9	2.8+/-0.7
15-20 cm	371	292+/-65	1.8+/-0.4	710+/-165	26.9+/-6.3	1.6+/-0.5	0.4+/-0.1
Contamination Density kBq/m^2		1178		194		32	

Table 5. *Characteristics of contamination within the soils of Site 4. Soil bulk density at Site 4 – 1.23 g/cm^3.*

Site 5

Site 5, N 51º47′11,8″ E 030º01′16,8″, was disturbed (ploughed to a depth of approx.30 cm) agricultural land exhibiting dose rates in the range 0.25 to 0.39 µSv/h at 1 m height (Table 6).

Layer	Layer Mass g	^{137}Cs Bq/kg	Percentage of ^{137}Cs in each layer	^{90}Sr Bq/kg	Percentage of ^{90}Sr in each layer	^{241}Am Bq/kg	Percentage of ^{241}Am in each layer
0-3 cm	340.2	2114+/-423	17.8+/-3.6			4.2+/-1.7	15.3+/-6.2
3-6 cm	287.8	2147+/-435	15.3+/-3.1			4.5+/-1.6	13.9+/-4.9
6-10 cm	385.0	2164+/-433	20.6+/-4.1			6.2+/-1.9	25.6+/-7.8
0-15 cm	450.6	2235+/-447	24.9+/-5.0			4.7+/-1.3	22.7+/-6.3
15-20 cm	478.6	1814+/-362	21.5+/-4.3			4.4+/-1.4	22.6+/-7.2
Contamination Density kBq/m^2		644				1.49	

Table 6. *Characteristics of contamination within the soils of Site 5. Soil bulk density at Site 5 – 1.55 g/cm^3.*

Figure 24. *Site 4 location from above and from ground level. Yellow line indicates 200 m scale.*

Figure 25. *Site 5 location from above and from ground level. Yellow line indicates 200 m scale.*

Site 6

Site 6 was a control site (Figure 26) where essentially no contamination, relative to the levels observed for the previous 5 sites, was to be found and was located outside the reserve within the nearby town of Khoiniki. Cs-137 levels at the site were 13 kBq/m^2 and 22 kBq/m^2 for ^{90}Sr.

Figure 26. *Site 6 location within the town of Khoiniki.*

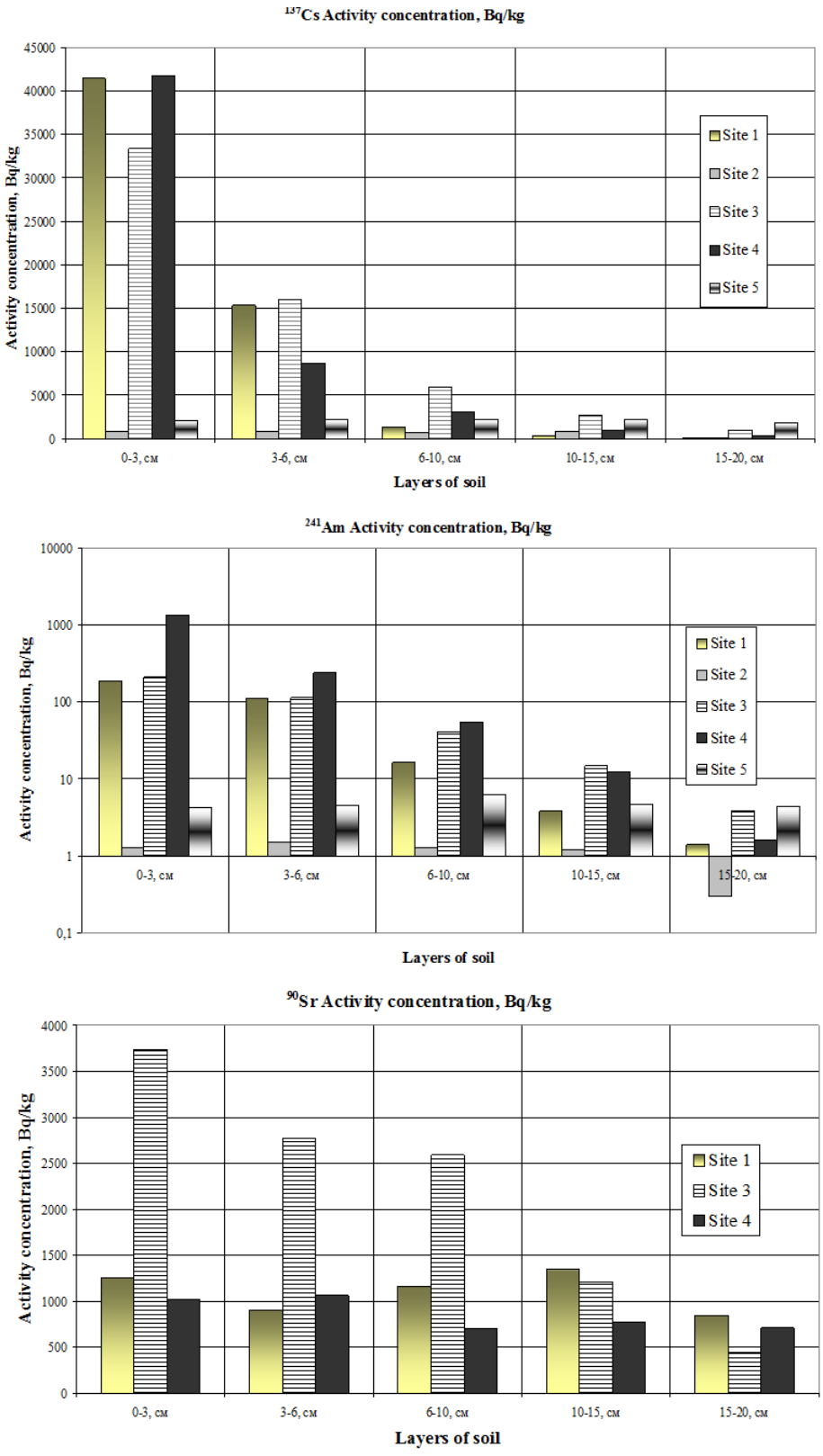

Figure 27. *Comparative depth distributions of ^{137}Cs, ^{241}Am and ^{90}Sr at all sites.*

The data presented in Tables 2 to 6 and Figure 27 of the vertical distribution of ^{137}Cs, ^{241}Am and ^{90}Sr in soil layers give an indication of the degree of contamination at selected sites by the aforementioned radionuclides. In the analysis of that data the following points could be noted. The behavior of ^{137}Cs, ^{241}Am on the sites 1, 3, 4 is "classical" (Drovnikov V.V. et.al., 2010). The major part of the activity is situated in the upper layers of soil. For example, at the 1st site (sod-podzol soil), 66 % of ^{137}Cs and 53 % of ^{241}Am occur in the layer 0-3 cm. The same situation is observed for Site 4 (flooded soil) - 57% and 66 % of ^{137}Cs and ^{241}Am respectively are found in layer 0-3 cm. It is interesting to note that in a peat soil (Site 3) the distribution of ^{241}Am between layers is the same as that of ^{137}Cs and the major part of these radionuclides occur in the first two layers over a depth of 0-6 cm rather than being confined to the layer 0-3 cm. In sandy soil (Site 2) the major part of ^{137}Cs and ^{241}Am has migrated deeper than 10 cm from the soil surface and the maximum activity corresponds to the layer 10-15 cm. In arable land (Site 5) the activity of ^{137}Cs and ^{241}Am in the three bottom layers, 6-20, cm is 1.5 times higher than that of the two upper layers. The layer 15-20 cm still contains about 22 % of ^{137}Cs and ^{241}Am. So in arable land not only ^{90}Sr but also ^{137}Cs and ^{241}Am could be located deeper than 20-30 cm. Sr-90 was not found at Sites 2 and 5. We suppose that this is due to the higher migration ability of ^{90}Sr in comparison with ^{137}Cs and ^{241}Am. On that basis, ^{90}Sr penetrates deeper than the 20 cm that is the extent of sampling in for GAMFAC. It was shown by Kashparov et al (2000) that for most sampling points, the main fraction of ^{90}Sr (more than 95 % of activity) is located in the 0-30 cm layer. Data accumulated on the distribution of ^{90}Sr along vertical soil profiles in the 30-km exclusion zone of the Chernobyl NPP show that in sandy soil as opposed to sandy loam, clay sand, sod-podzol and peat soil, a substantial fraction of ^{90}Sr has already migrated deeper than 30 cm (Lujanieneo et.al., 2002). With repeated ploughing of the soil on the cropland (Site 5), ^{90}Sr also probably could be able to migrate below than 20 cm. In sod-podzol and flooded sites, the maximal activity of ^{90}Sr corresponds to the layer 10-15 cm. In peat soil the peak of ^{90}Sr activity falls within the layer 6-10 cm.

The occurrence of the peaks in activity of the radionuclides is explained by the peculiarities of vertical migration of radionuclides in the corresponding types of soil. Convective transport and diffusion are the main processes of vertical migration of radionuclides in soil. These processes are characteristic for water-soluble and, partially, for exchangeable species of radionuclides in soil. Counteraction of these two processes - convective transport and molecular diffusion - together with peculiarities of the physicochemical properties of the soil is the main reason for the occurrence of the above mentioned peaks of activity of

radionuclides. It is worth noting the substantial difference between levels of radioactive contamination of Sites 1 and 2. These sites are close to each other – the distance between them is only 200-250 m. But the difference in the density of surface contamination is higher than one order of magnitude for ^{137}Cs. In case of ^{241}Am that difference is still higher. This is an example of the high inhomogeneity of radioactive contamination of the territory of exclusion zone of Chernobyl NPP.

4.0 Results and Discussion

4.1 Norwegian Radiation Protection Authority, Norway

Site 1 had a soddy-podzol soil type and, based on the soil core results, an exponential model with relaxation length between 2.0 cm and 4.0 cm and soil density between 1.47 and 1.77 g/cm3 was assumed. A comparison between layer measurements of the soil core samples and the two exponential models is displayed in Figure 28.

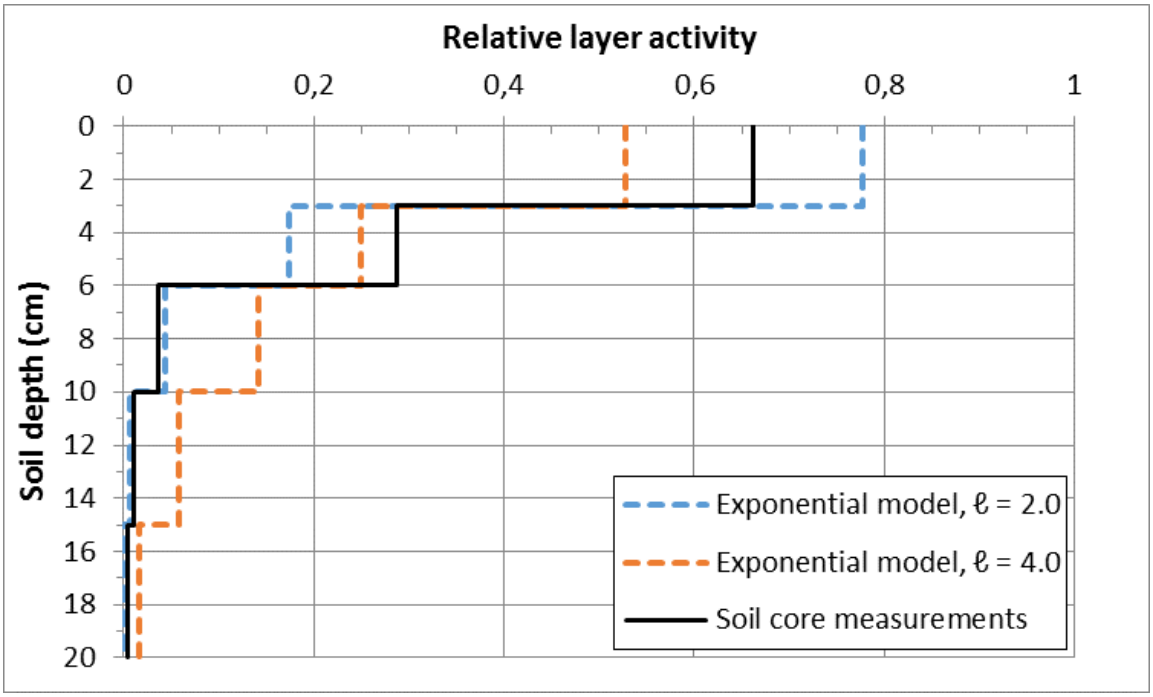

Figure 28. *Exponential activity depth distribution modelling for Site 1.*

The above assumptions for the depth distribution gives calculated activity concentration results as shown in Table 7. The average dose rate measured at this site was 2.28 µSv/h.

Detector	Activity (kBq/m^2)	95 % C.I.
CZT	2130	1440-2820
NaI	2210	1580-2840

Table 7. *Calculated results for the activity best estimate and 95 % confidence interval (C.I.) at Site 1.*

Site 2 exhibited a sandy soil type with high penetration of contamination. Slab model with thickness between 12.0 cm and 16.0 cm was assumed, with soil density between 1.62 g/cm^3 and 1.92 g/cm^3. These assumptions for the depth distribution gives calculated activity concentration results as shown in Table 8. The average dose rate measured at this site was 0.25 µSv/h.

Detector	Activity (kBq/m^2)	95 % C.I.
CZT	180	100-270
NaI	200	140-260

Table 8. *Calculated results for the activity best estimate and 95 % confidence interval (C.I.) at Site 2.*

For the peat soil of Site 3 an exponential source model was assumed, with relaxation length 4.5 and 8.5 g/cm3, density from 1.0 to 1.3 g/cm^3. A visual comparison of the model with the measured relative activities of the soil core layer is displayed in Figure 29.

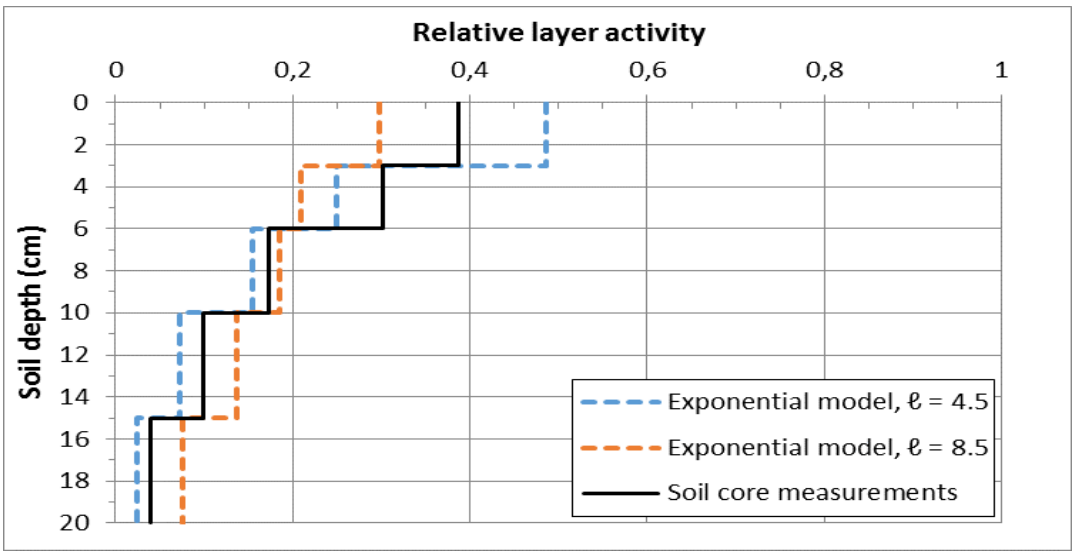

Figure 39. *Exponential activity depth distribution modelling for Site 3.*

The above assumptions for the depth distribution gives calculated activity concentration results as shown in Table 9. The average dose rate measured at this site was 1.76 µSv/h.

Detector	Activity (kBq/m^2)	95 % C.I.
CZT	1760	1110-2420
NaI	1960	1310-2600

Table 9. *Calculated results for the activity best estimate and 95 % confidence interval (C.I.) at Site 3.*

Site 4 floods with water from a nearby river at certain times during the year. An exponential model was assumed, with relaxation length between 2.5 cm and 5.0 cm and density between 1.08 and 1.38 g/cm^3. A comparison between the model and soil layer measurements is presented in Figure 40.

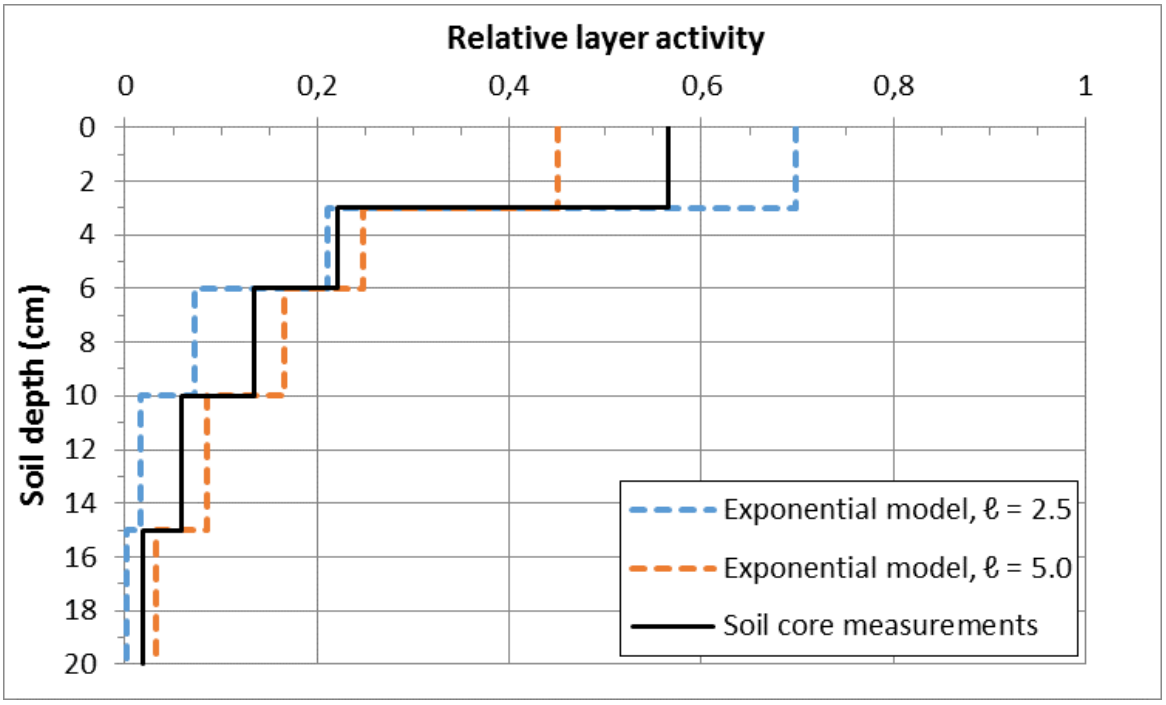

Figure 40. *Exponential activity depth distribution modelling for Site 4.*

The above assumptions for the depth distribution gives calculated activity concentration results as shown in Table 10. The average dose rate measured at this site was 0.94 µSv/h.

Detector	Activity (kBq/m^2)	95 % C.I.
CZT	810	490-1130
NaI	730	430-1030

Table 10. *Calculated results for the activity best estimate and 95 % confidence interval (C.I.) at Site 4.*

Site 5 exhibited uniform distribution down to at least 20 cm; however, since this soil has been cultivated using a plow an even deeper distribution cannot be disregarded. Therefore, the slab thickness was assumed to be between 20.0 cm and 30.0 cm, with density ranging from 1.4-1.7 g/cm^3.

The above assumptions for the depth distribution gives calculated activity concentration results as shown in Table 11. The average dose rate measured at this site was 0.28 μSv/h.

Detector	Activity (kBq/m^2)	95 % C.I.
CZT	570	290-850
NaI	610	340-880

Table 11. *Calculated results for the activity best estimate and 95 % confidence interval (C.I.) at Site 5.*

The control site, Site 6, was a football pitch near Khoiniki town. As this site had not been previously characterized with regards depth distribution and soil density, and time at the site was limited, proper activity computations could not be made. However, the observed photopeak count rates indicate an activity concentration for ^{137}Cs of around the order of 10 kBq/m^2, which is close to the MDA of the CZT setup.

A comparison of the calculated activity of ^{137}Cs from all five sites is shown in Table 41. Results from both the CZT and the NaI detector systems are displayed together with results from the analysis of soil core layers performed by the PSRER laboratories. The error bars in the blue and red columns correspond to the 2σ uncertainty in the CZT and NaI measurements, respectively. While uncertainty values for the soil core measurements were not explicitly reported, a general estimate of 20-30 % relative uncertainty is expected.

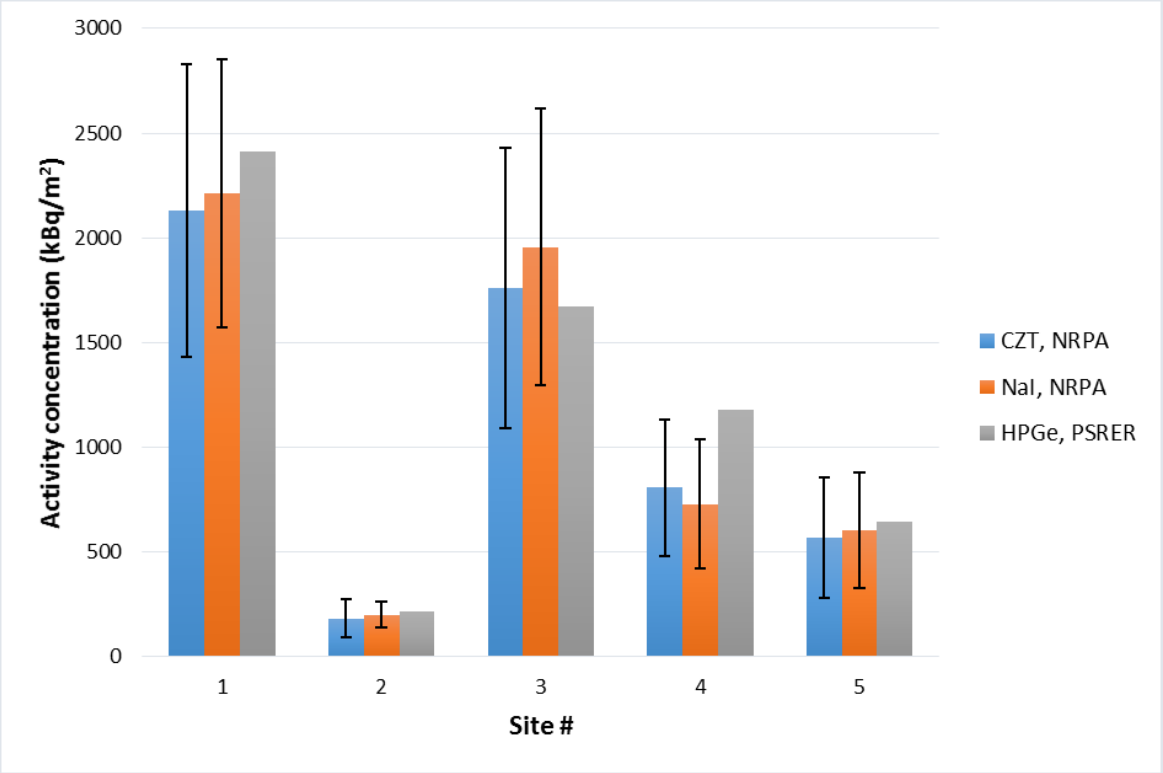

Figure 41. *Comparison of calculated activity results from the two detector systems with previous site characterization performed by PSRER using soil core measurements. Error bars correspond to a 2σ uncertainty level.*

Both the CZT and NaI detector setups provide good fit-for-purpose systems for in situ gamma spectrometric measurements of a potentially contaminated site. The portability of the systems, combined with the fast setup time, means that measurements can start within minutes of arriving at a site. In addition, using detectors with small crystals and/or fast decay times is essential when trying to characterize heavily contaminated sites as, for example, large HPGe detector systems will often saturate at contamination levels above a few MBq/m^2. The largest

dead times we observed with our detector systems was at Site 1 (dose rate 2.3 µSv/h) with approximately 4 % dead time for the NaI system and 0.3 % dead time for the CZT system.

The calculated results indicate that accuracy and precision in the measurements is satisfactory for this type of application. Results from both systems are in good agreement with each other, as well as with the soil core measurements. Site 4 is the only site where the measured activity from in situ systems seems to be significantly different from the sample measurements. The reason for this does not seem immediately apparent, however the fact that this site is partly impounded means that it is a challenging site to characterize as there may be significant temporal variations in the soil and vegetation properties. Detector calibrations will also have an impact on the results. As both the CZT and NaI detectors were calibrated using the same source set, the measurements are somewhat prone to systematic effects. In addition, site 4 appeared to be the most inhomogeneous of the five sites. With only three separate measurements within the grid it is possible that a hot spot was missed. In any case, the observed agreement is acceptable for this type of application.

While the activity calculations we performed for this exercise were limited to measurements of ^{137}Cs, the assessment of other gamma-emitting radionuclides should be possible with the current detector setup. On the more contaminated sites, clear peaks were observed at approximately 32 keV and 37 keV in the CZT spectra, corresponding nicely to the xK energies of ^{137}Ba. This indicates that the CZT detector could even be used to measure lower energy emitters, and is an interesting application for further development. Currently, CZT detectors are not widely applied for in situ gamma site characterizations, although they have been used by Japanese researchers for measuring sites contaminated after the Fukushima Daiichi incident (Kowatari et al, 2015).

One of the most crucial factors for successful in situ gamma spectrometric site characterizations is to have good, operative procedures that can be employed in the case of an emergency scenario involving contamination with radiological or nuclear agents. Participating in field exercises is one of the best ways to ensure that technical skills are maintained and that the equipment operates as expected. In our opinion, the GAMFAC exercise proved very effective in this respect.

4.2 Swedish Defence Research Agency, Sweden

According to the information that was provided for Site 1, ^{137}Cs, ^{90}Sr and ^{241}Am should be present in the area. The measurements at site 1 showed a strong peak at 662 keV, which is the key signature of ^{137}Cs. Two small peaks at 68 and 78 keV could also be seen. These two peaks are most likely x-rays from gold which originate from inside the instrument. Gold is used along aluminum components inside the detector to protect against corrosion. Apart from that, a backscatter peak and the Compton edge from the 662 keV peak and a peak at 1461 keV from ^{40}K, are also distinguishable (Figure 42).

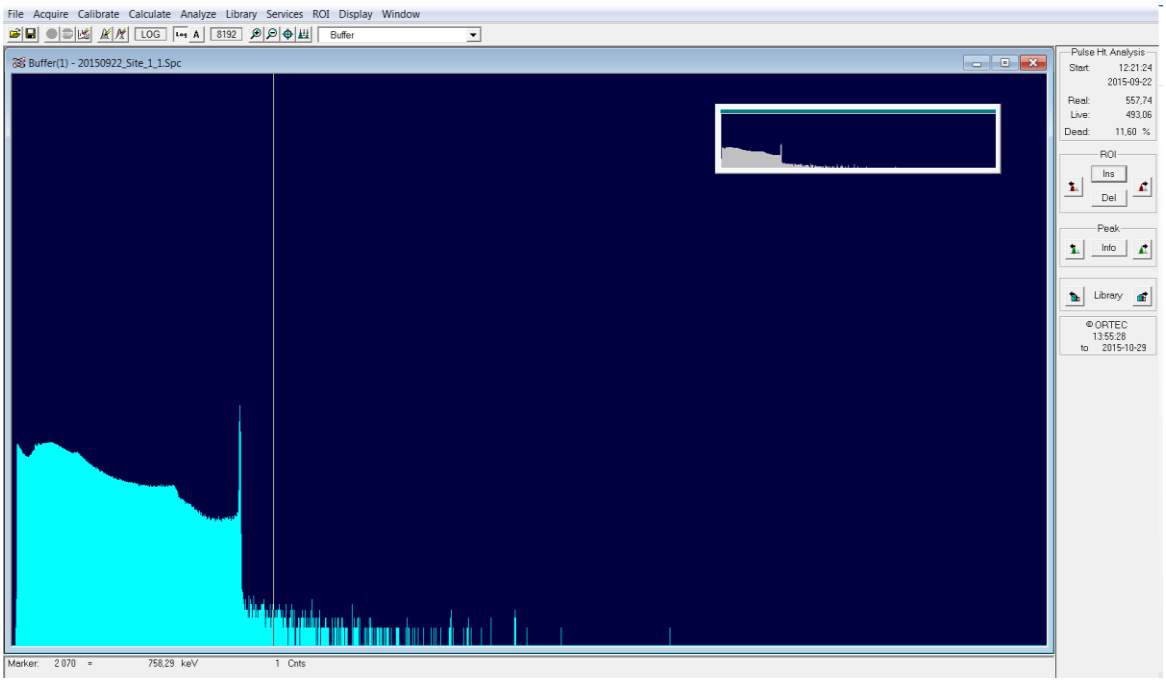

Figure 42. *Example of a gamma spectrum from measurements at Site 1.*

Calculations of the activity concentration in the soil showed that the equivalent surface activity model and the model for emergency preparedness underestimated the concentration of ^{137}Cs more than 5 and 3 times respectively. This was due to the fact that the models don't account for that at least 35 % of the activity is below the 2 cm of top soil. The exponential model on the other hand gave an activity concentration in the soil that was within 30 % of the concentration that was calculated from laboratory measurements (Table 2). The ambient dose rate equivalent was 1.8 µSv/h at site 1 (Table 12).

Model	Activity ^{137}Cs (Bq/m^2) *In situ*	Activity ^{137}Cs (Bq/m^2) Lab. measurement	Dose rate (µSv/h)	
			Detective Ex	Polimaster
Equivalent surface activity	4.3 x 10^5	2.4 x 10^6	1.81	1.85
Emergency preparedness	6.4 x 10^5			
Exponential dist. (10 cm)	3.1 x 10^6			

Table 12. *Dose rate and activity at Site 1.*

At Site 2 the area should contain ^{137}Cs and ^{241}Am according to the information provided. The measurements at Site 2 showed a similar pattern as at Site 1. The ^{137}Cs 662 keV peak as well as the gold x-ray peaks and the 1461 keV peak from ^{40}K were visible. The backscatter peak and the Compton edge were not as distinct as at site 1. No peak related to ^{241}Am could be distinguished (Figure).

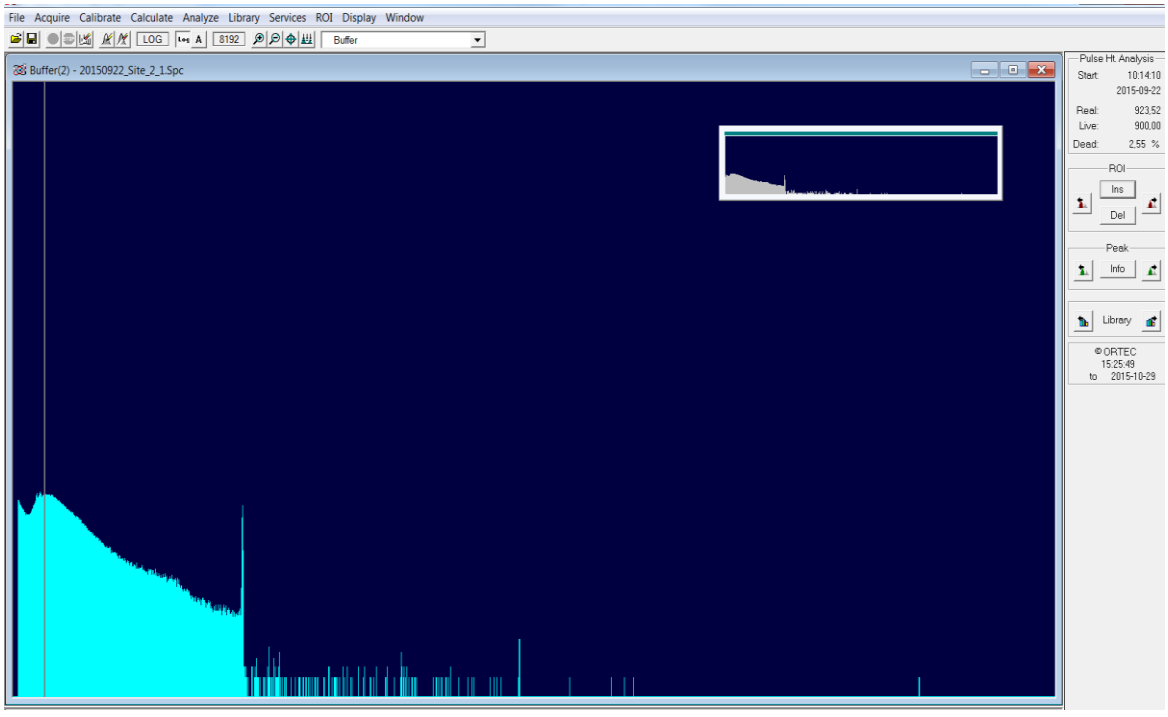

Figure 43. *Example of a gamma spectrum from measurements at Site 2.*

Calculations of the activity concentration in the soil showed that the equivalent surface activity model and the model for emergency preparedness underestimated the concentration of

^{137}Cs more than 10 and 7 times respectively. At Site 2 at least 75 % of the activity is below the 2 cm of top soil. The uniform distribution model gave an activity concentration in the soil that was within 5% to the concentration that was calculated from laboratory measurements (Table 3). The ambient dose rate equivalent was 0.25 µSv/h (Table 13).

Model	Activity ^{137}Cs (Bq/m^2) *In situ*	Activity ^{137}Cs (Bq/m^2) Lab. measurement	Dose rate (µSv/h) Detective EX	Dose rate (µSv/h) Polimaster
Equivalent surface activity	2.0 x 10^4	2.2 x 10^5	0.26	0.25
Emergency preparedness	3.0 x 10^4			
Uniform dist. (20 cm)	2.1 x 10^5			

Table 13. *Dose rate and activity at Site 2.*

No measurements were performed at Site 3 since the battery of the instrument was exhausted and there was no time to recharge it.

Site 4 should contain ^{137}Cs, ^{90}Sr and ^{241}Am according to the information to hand. The pattern was similar as the other sites. A pronounced 662 keV peak from ^{137}Cs as well as the 1461 keV ^{40}K peak and the small peaks from gold x-rays could be seen. The Compton edge and backscatter peak from 662 keV were also clearly visible. No peak from ^{241}Am could be seen (Figure 44).

The activity at Site 4 showed the largest discrepancy between the different measurement points. The count rate differed almost twice between the measurements. The distribution model that gave results close to the lab measurements was the exponential model, within 3% (Table 14).

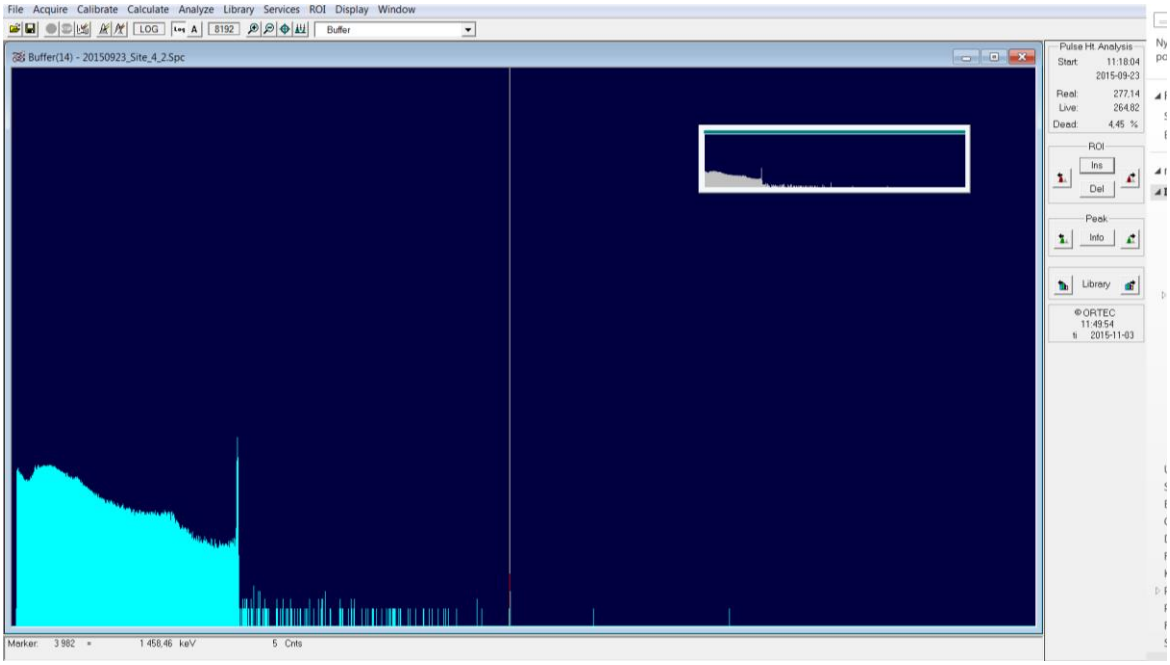

Figure 44. *Example of a gamma spectrum from measurements at Site 4.*

Model	Activity ^{137}Cs (Bq/m^2) *In situ*	Activity ^{137}Cs (Bq/m^2) Lab. measurement	Dose rate (µSv/h) Detective EX	Dose rate (µSv/h) Polimaster
Equivalent surface activity	1.6 x 10^5	1.2 x 10^6	0.74	0.68
Emergency preparedness	2.4 x 10^5			
Uniform dist. (20cm)	1.2 x 10^6			

Table 14. *Dose rate and activity at Site 4.*

At Site 5 ^{137}Cs and ^{241}Am were indicated in the lab measurements. As at the other sites the measurements showed only ^{137}Cs and ^{40}K related peaks, plus the x-rays from gold inside of the detector. The activity calculations from Site 5 showed a larger discrepancy as compared to the results from the lab measurements even with the model that was closest to the lab data (Table 15). According to the information from the lab measurements, the activity is evenly distributed down to 20 cm and no data from below 20 cm is available. The ambient dose rate equivalent at site 5 was 0.2 µSv/h.

Model	Activity ^{137}Cs (Bq/m^2) *In situ*	Activity ^{137}Cs (Bq/m^2) Lab. measurement	Dose rate (µSv/h) Detective EX	Polimaster
Equivalent surface activity	3.2 x 10^4	6.4 x 10^5	0.21	0.27
Emergency preparedness	4.9 x 10^4			
Uniform dist. (20 cm)	3.5 x 10^5			

Table 15. *Dose rate and activity at Site 5.*

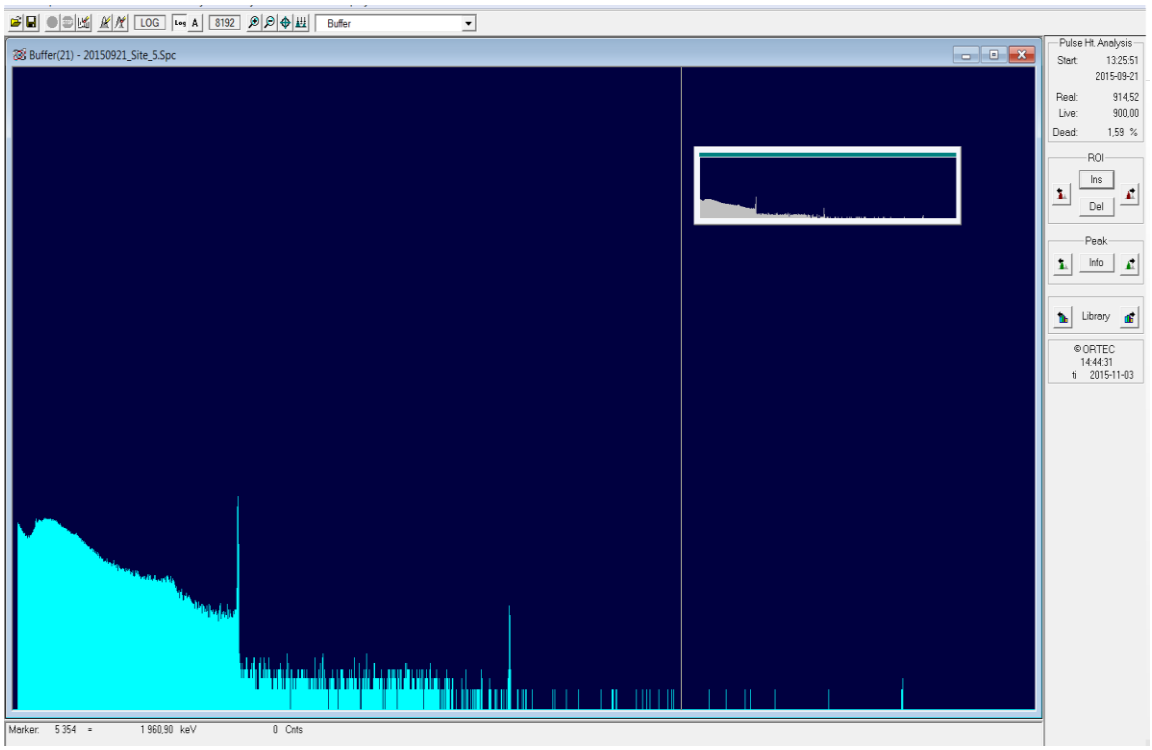

Figure 45. *Example of a gamma spectrum from measurements at Site 5.*

Site 6 was the control site, with little contamination from the Chernobyl accident. It was a soccer field in the town of Khoiniki. The spectrum from this site, also showed a marked ^{137}Cs peak at 662 keV and the ^{40}K peak at 1461 keV. There was also peaks from natural background as the 609 keV ^{214}Bi peak and the ^{208}Tl peak at 2615 keV. The activity calculations with the exponential model gave results that were close to, within 8%, the laboratory measurements (Table 16).

Model	***Activity ^{137}Cs (Bq/m^2) In situ***	***Activity ^{137}Cs (Bq/m^2) Lab. measurement***	***Dose rate (µSv/h)***	
			Detective EX	*Polimaster*
Exponential dist. (10 cm)	1.4×10^4	1.3×10^4	0.21	0.27

Table 16. *Dose rate and activity at Site 6.*

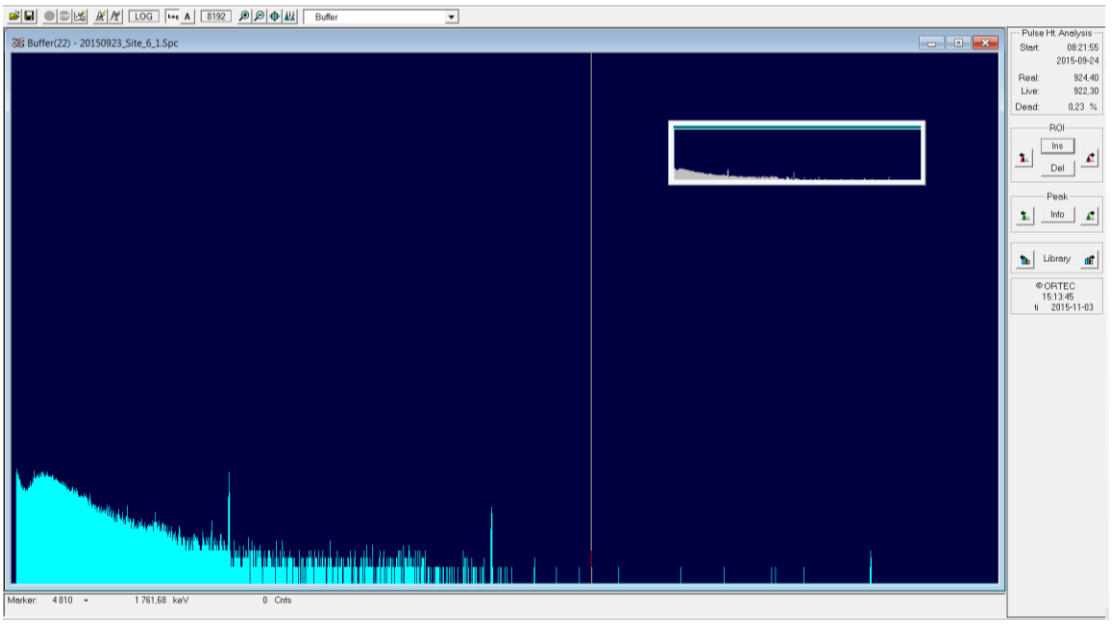

Figure 46. *Gamma spectrum from measurement at Site 6.*

4.3 Danish Emergency Management Agency, Denmark

The results of DEMA calculations are summarized in Table 1 and in Figure 47. It is seen that there in general is a good agreement between the activity concentrations calculated by DEMA using ISOCS and the measurements of soil samples made by Polessie State Reserve. However, the data indicate that there at some sites is an inhomogeneous distribution of ^{137}Cs in the ground. This is especially the case at Site 4 where DEMA measures activity concentrations between 663 and 2158 kBq/m^2. Altogether, it is shown that ISOCS sourceless calibration software is a useful tool in in-situ gamma spectrometry and that the distribution models used in this study can be used to obtain meaningful activity concentration for contaminated sites after nuclear accidents.

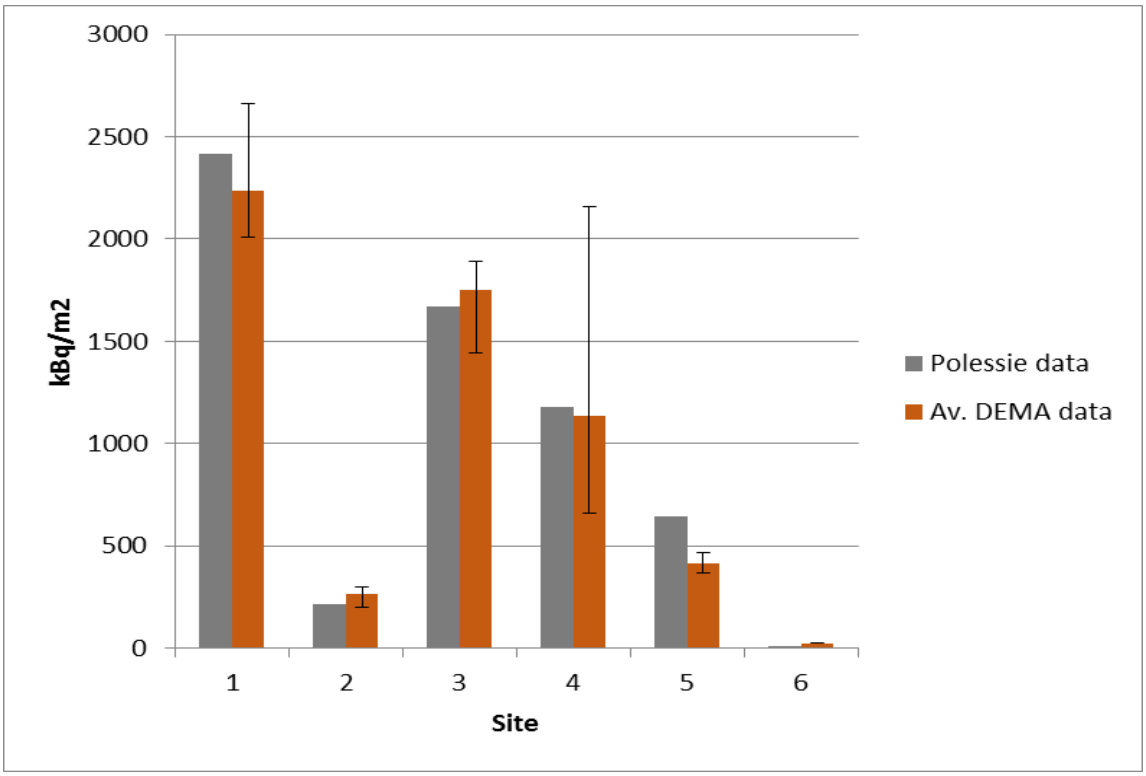

Figure 47. *Average ^{137}Cs activity concentration (kBq/m^2) for each of the 6 sites compared to the Polessie data from soil samples. The full variation of the data is shown as error bars.*

4.4 Stirling University, Scotland

In situ results for both instruments were within an acceptable activity range of core results at Sites 1, 2 and 4 (Table 17). However, at Sites 3 and 5 significant deviation was found. This source of error was most likely to have been a calibration error or an anomalous measurement. Another factor could also have been heterogeneity in ^{137}Cs activity and depth distribution across individual sites. Notice that the uncertainty associated with LaBr:Ce estimates is slightly less than the NaI:Tl owing to LaBr:Ce increased energy resolution and efficiency. Dose rates across the measured sites would appear to change alongside ^{137}Cs activity. Notice the system reached overload at Site 3 (Table 18).

	Site 1	Site 2	Site 3	Site 4	Site 5
Sodium iodide	2399 ± 253	303 ± 202	2031 ± 221	917 ± 196	280 ± 210
Lanthanum bromide	1711 ± 250	205 ± 86	1049 ± 207	-	226 ± 35
Soil cores	2444	215	1672	1178	644

Table 17. *Activity estimates for the 5 sites*

	Site 1	Site 2	Site 3	Site 4	Site 5
Dose rate	1.737 ± 0.013	0.226 ± 0.013	Overload	1.092 ± 0.056	0.212 ± 0.012

Table 18. *Effective dose rates for individual sites*.

To assess the heterogeneity of individual sites mobile data acquired from the exclusion zone was mapped. Only LaBr:Ce data is presented here as it was as NaI:Tl data was affected by spectral drift. The difference in activity across the sites is captured well using the remote survey (Figure 48). Median values are in good agreement with activities described by soil cores. Additional information regarding α values provides good insight into the relative depth of the source at each site. Notice how variation across the sites is quite different. For example, the highest activity site (Site 1) did not exhibit a large amount of variation in both depth and activity and the activity was mainly associated with the surface of the soil profile (α = 0.2). Minimal variation can be seen spatially by observing the mapped distribution of activity and depth for Site 1 (Figure). The majority of the sites remains between 2500 and 3500 kBq m^{-2}. Site 4, on the other hand, exhibited the largest amount of variation in both depth (α = 0.05-0.5) and activity (50-3100 kBq m^{-2}). Interestingly, this could possibly be attributed to inundation of water from a nearby lake and river system potentially removing some of the

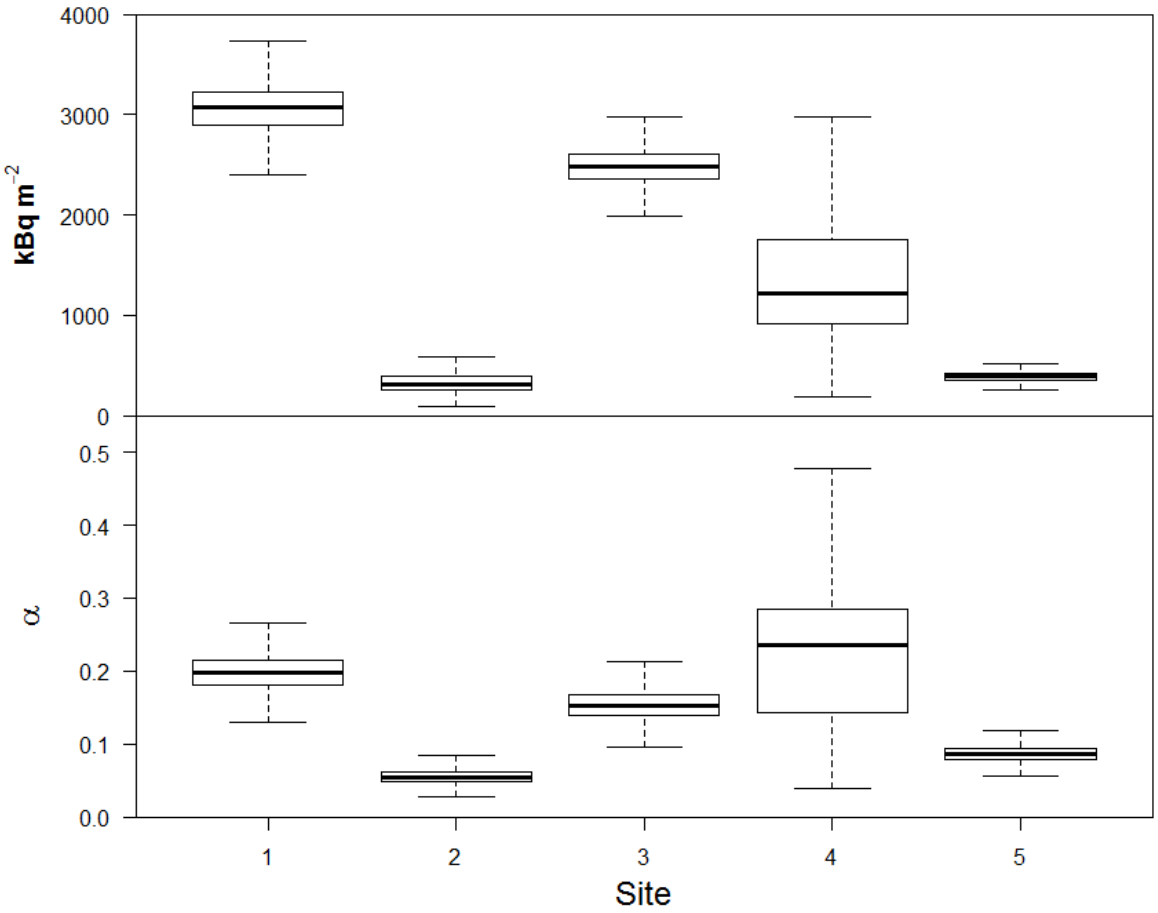

Figure 48. *Activity and depth values (α) for lanthanum bromide mobile survey of the individual sites.*

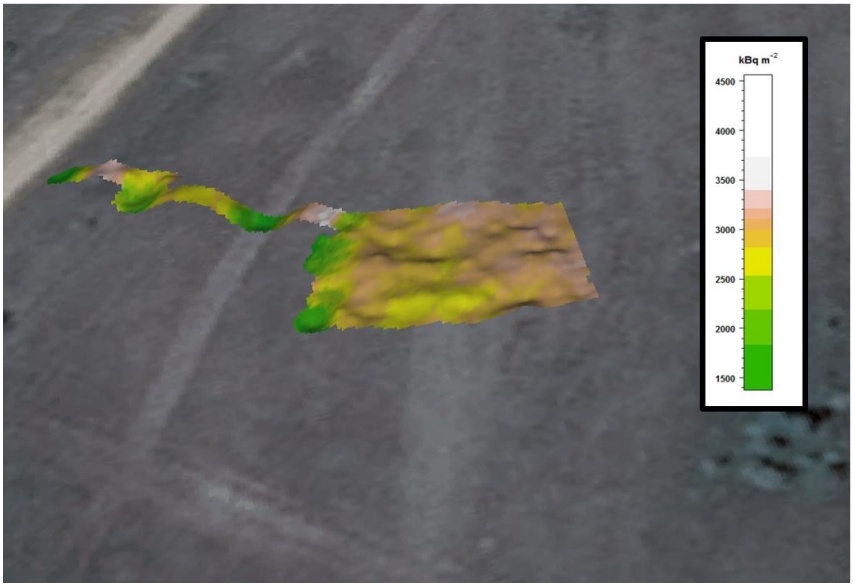

Figure 49. *Spatial distribution of activity for Site 1.*

activity and/or driving it deeper into the soil column. This is evident in Figure 50, in which there is markedly a lower activity, at a greater depth, near towards the shore of the lake and in a topographically lower part of the site. Further away from the lake and higher up, much greater activities can be encountered closer to the surface. Another spatially interesting site is Site 2 (Figure 51). During investigations, a clear peak could be identified to the north of the site. After mapping, it become clear this is an area of higher activity that is slightly higher in the soil column compared to surrounding areas.

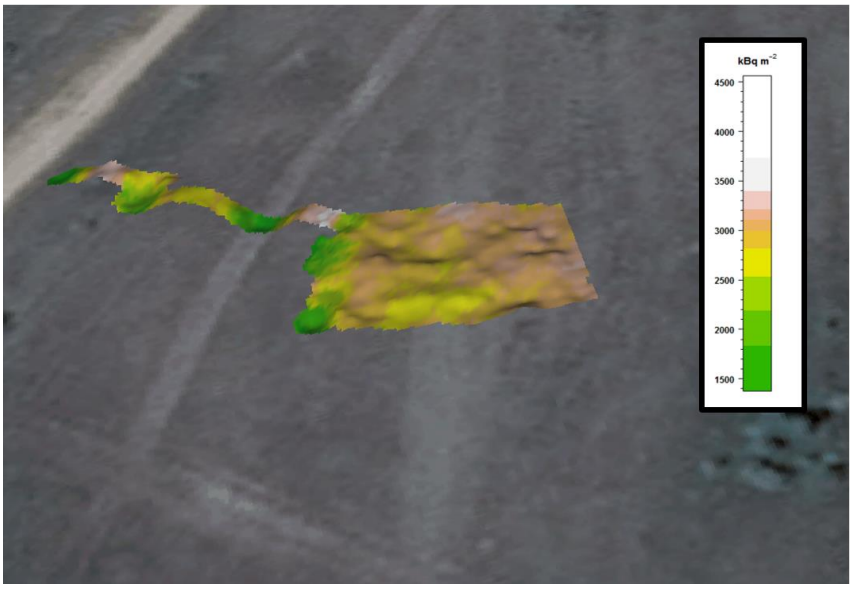

Figure 49. *Spatial distribution of activity for Site 1.*

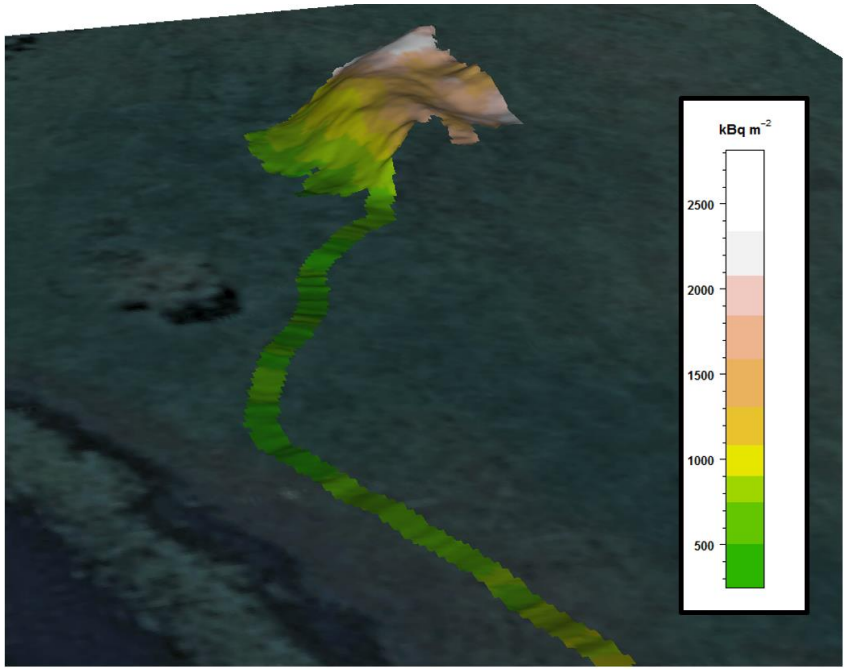

Figure 50. *Spatial distribution of activity for Site 4.*

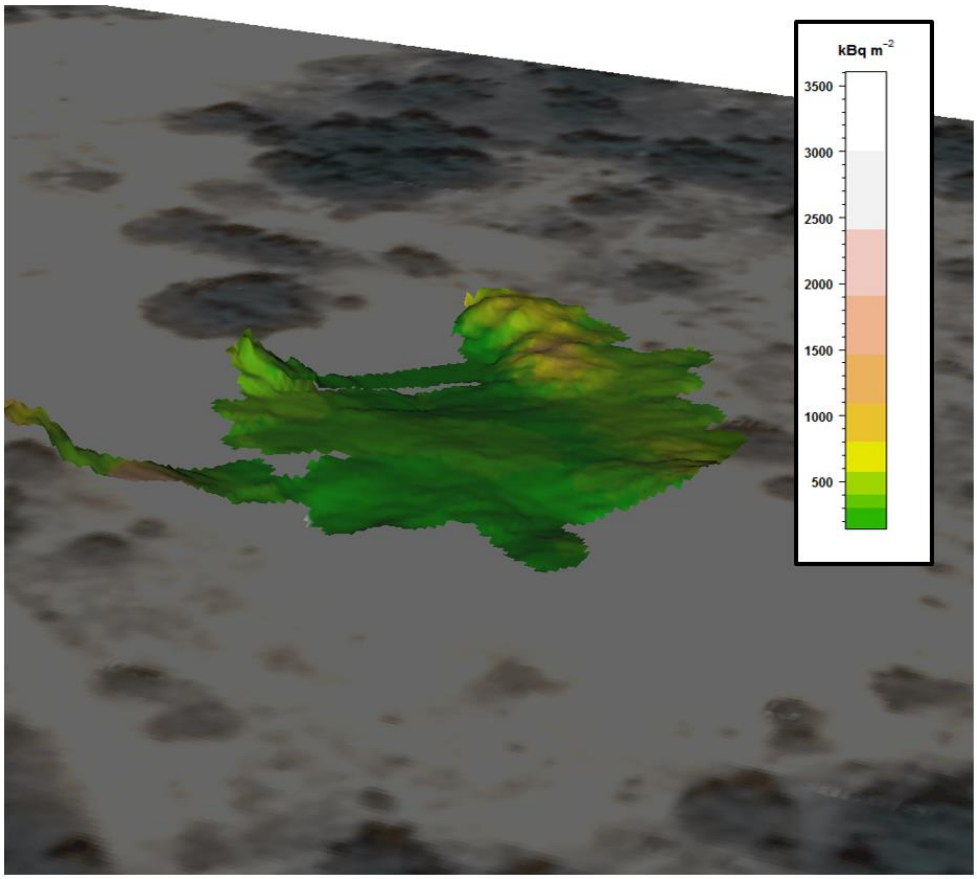

Figure 51. *Spatial distribution of activity for Site 2.*

Overall the SMoGSS system performed well across the study areas operating within the in-situ and mobile phases. The sodium iodide detector tended to have a larger dead time (10%) compared with the lanthanum bromide (5%). In addition the inability to process the high count rates effectively resulted in a summation peak at 1324 keV (2 x 662 keV) in the sodium iodide spectra (Figure 52) which can be observed to the left of the ^{40}K peak at channel 440. There is evidence that this affected the sodium iodide detector, which is routinely gain stabilised on the ^{40}K peak, resulting in some noticeable spectral drift, illustrated by the small shift in the ^{137}Cs peaks with higher count rates in Figure 52. Although not explicitly tested, the DPGS operated well across each study site enabling the activity and depth distribution of ^{137}Cs to be mapped. Within the Polessie State Radiation Ecology Reserve, 76 x76 mm size detectors operated well. Long count times were unnecessary and activity and depth distributions were obtained. In the mobile mode, the SMoGSS system was able to map the ^{137}Cs inventory and depth distribution with a minimum of 1200 one second spectra acquired

across each site. This enables systematic patterns of ^{137}Cs activity and depth variation to be mapped, as shown clearly at Sites 2 and 4. The high count rates impacted more on the sodium iodide detector than the lanthanum bromide detector resulting in a greater dead time and spectral drift as a result of coincidence counting interfering with the gain stabilization.

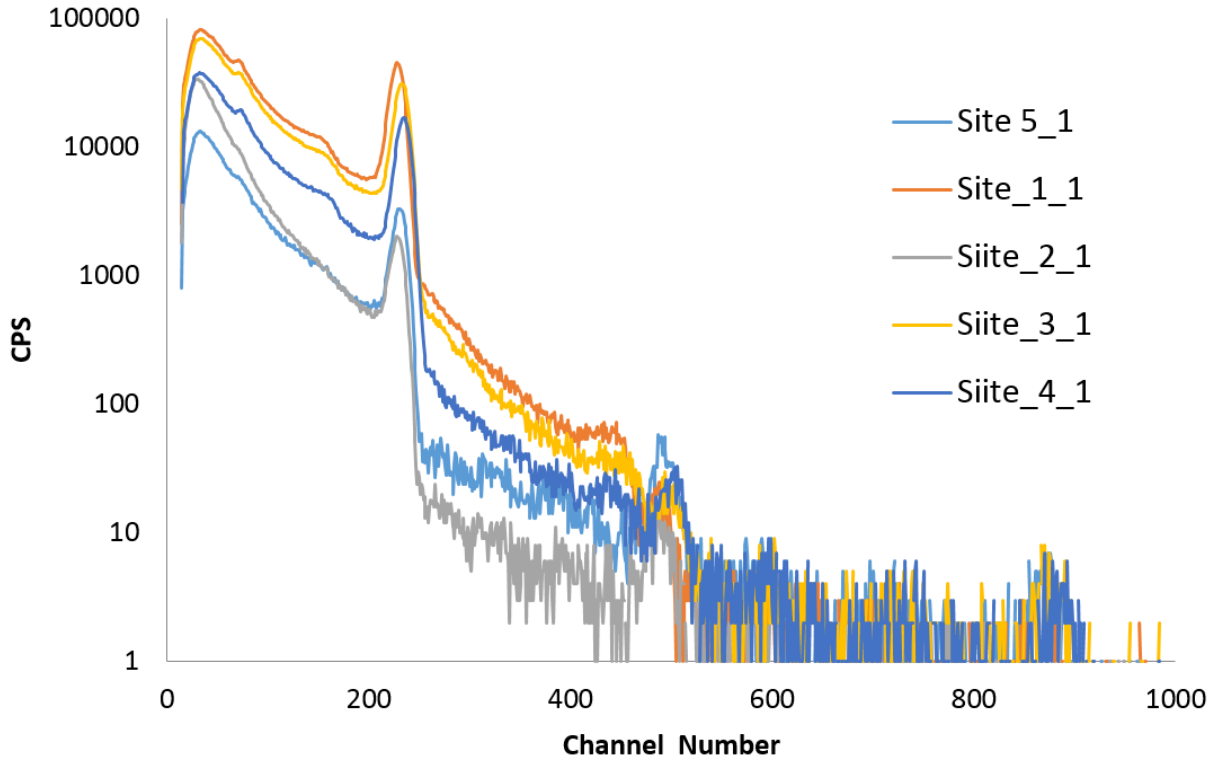

Figure 52. *Sodium Iodide spectra acquired at each site.*

4.5 Icelandic Radiation Protection Authority, Iceland.

Results from the Icelandic team are shown in Table 19. Information from measurements of soil samples were used to determine the depth distribution. For sites 1, 3 and 4 exponentially decreasing depth distribution was assumed with relaxation depths of 2,8 cm, 7,5 cm and 5,3 cm respectively. For sites 2 and 5 a uniform slab distribution was assumed, with slab thickness of 15 cm and 20 cm respectively. No uncertainty was used for the soil density or the vertical source distribution so the overall uncertainty is underestimated.

The results from all the sites are reasonably near the values given from soil measurements, except the results from Site 4. At site 4 the Icelandic results give almost 1.000 kBq/m^2 more than the soil measurements.

Differences between results from in-situ measurements and soil sample measurements could perhaps be partially explained by the presence of vegetation on the ground, which is typically removed from soil samples during sample processing. The results were calculated using the InSiCal program written and provided by Alexander Mauring at the NRPA.

No distinct peaks from ^{241}Am were seen in the spectra from any of the sites: the low energy peaks were not detectable through the scatter from ^{137}Cs. At sites 1 and 4 small peaks from ^{154}Eu were identified but not quantified. It is theoretically possible to determine the vertical source distribution with in-situ measurements, for example with different measurement distances or measurements at different angles but it would have been too time consuming in the context of this project, and some kind of a collimator would have been needed in some instances.

The Icelandic team made some measurements using different distances from the ground surface, from 0.5 m to 1.85 m, at Site 4. The results did not indicate a significant difference related to distance. For the ^{137}Cs peak the optimum measurement distance in practical application for calculating the vertical source distribution is estimated to be 1-10 meters [chapter 2.4.1, High resolution Field gamma spectrometry, Robert R. Finck].

Site #	Source distribution	[kBq/m^2]	[± kBq/m^2]	Detector dead time	Given values for ^{137}Cs [kBq/m^2]
1	Exponential	2,472	113	20,8	2,414
2	Slab	292	13	5,1	215
3	Exponential	2,583	121	17,5	1,672
4	Exponential	960	45	9,0	1,178
5	Slab	583	26	3,3	644

Table 19. *Calculated contamination with ^{137}Cs.*

During transportation between the sites the detector system was strapped in a seat of the bus at approximately 2.5 meters height above ground level. A job file in GammaVision was used to make continuous 10-second spectra. It took GammaVision 3-4 seconds to save the data after the end of each measurement so the interval between data points is 13-14 seconds. The results from these mobile measurements are shown in Figure 53. The figure shows the dose

rate in µSv/h. The dose rate conversion factor was calculated by using the measured dose from a handheld detector (RadEye G-10) based on the sum of counts from 30-3000 keV in HPGe spectra.

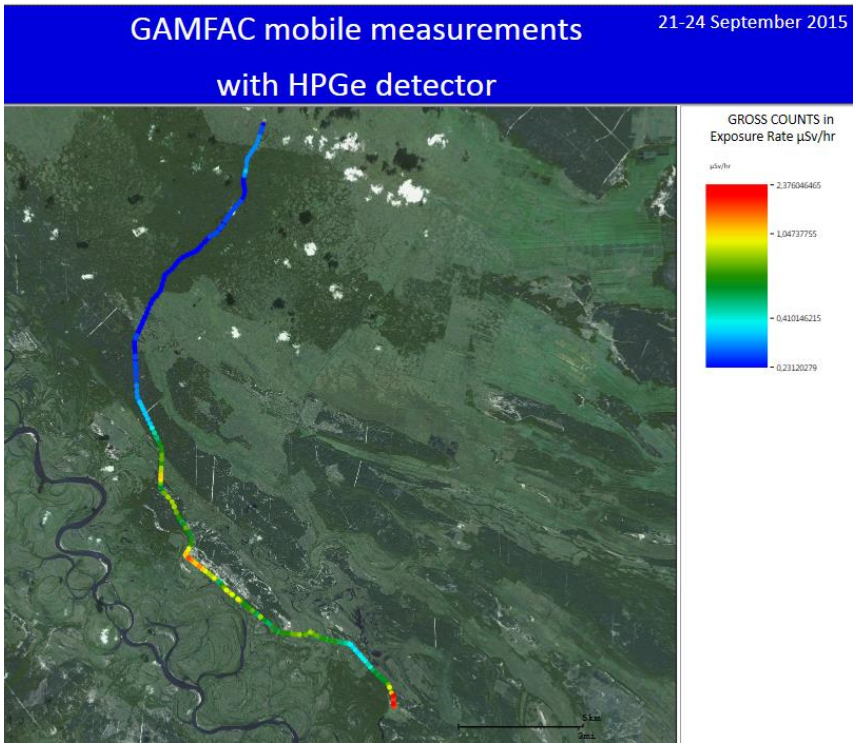

Figure 53. *Depiction of mobile measurement data obtained using GammaVision.*

5. Overall Conclusions

The GAMFAC activity provided a useful opportunity test both teams, equipment and procedures for making in-situ measurements in a testing environment. The sites available for testing varied substantially in terms of contamination density, soil type and landscape, depth penetration and geographical context. The suite of equipment deployed for making the measurements was impressive ranging from the smallest CdZnTe detector to much larger HPGe and NaI detectors all utilizing a wide array of ancilliary instrumentation and data processing equipment. It was noted that the ability of a team to successfully conduct such measurements is largely related to the amount of work and preparation invested in calibration and procedure development prior to the actual exercise. While it is possible to generate data from relatively simple procedures it was noted that incorporation of factors such as soil density and selecting the best models to describe the downward migration of radionuclides

significantly improved the estimates of activity deposition. Acceptable agreement between in-situ estimates and laboratory determinations were observed where *a priori* calibrations and routines had been devised and implemented. All detector types appeared to perform equally well, no significant advantages being reported in relation to the intrinsic performance characteristics of the detectors. Practical advantages and disdvantages were of course observed primarily in relation to size, weight and the cooling options utlilised for the various semi-conductor detectors employed. A novel means of mapping and determining depth distributions was demonstrated with evident advantages in terms of the type and quantity of information that can be generated using typical in-situ measurement setups.

References

Beck, H.L., DeCampo, J., Gogolak, C., 1972. *In situ* Ge(Li) and NaI(Tl) gamma-ray spectrometry, HASL-258, Health and Safety Laboratory, U.S. Atomic Energy Commission, New York, New York.

Boson J., Plamboeck A. H., Ramebäck H., Agren G., Johansson L., 2009. Evaluation of Monte Carlo-based calibrations of HPGe-detectors for in situ gamma-ray spectrometry. J. Environ. Radioact. 100 (11) 935-40.

Briesmeister, J. F., MCNP-A general purpose Monte Carlo code for neutron and photon ... Los Alamos National Laboratory, Los Alamos, New Mexico, 1993.

Drovnikov V.V., Egorov M.V., et.al. New method of determination of activity of gamma radiation sources situated behind layer of the absorber with a priory known properties – Method of G-factor. ANRI. 2010. No 3 (62). P. 9-15. In Russian.

Finck R.R., 1992. High resolution field gamma spectrometry and its application to problems in environmental radiology. Dissertation at Malmö department of radiation physics.

Helfer I.K., Miller K.M., 1988. Calibration factors for Ge detectors used for field spectrometry. Health Phys. 53, 365-380.

ISO 18589-7:2013, 2013. Measurement of radioactivity in the environment – Soil – Part 7: In situ measurements of gamma-emitting radionuclides, International Organization for Standardization, Genève.

Kashparov V.A., Lundin S.M., Homutinin Yu.A., et.al. Contamination by ^{90}Sr of the territory of near zone of Chernobyl NPP. Radiochemistry. 2000. Vol. 42, No 6. P. 550-559. In Russian.

Kowatari, M., Kubota, T., Shibahara, Y., Fujii, T., Fukutani, S., Takamiya, K., Mizuno, S., Yamana, H., 2015. Application of a CZT detector to *in situ* environmental radioactivity measurement in the Fukushima area, Radiation Protection Dosimetry, 2015 May 6. pii: ncv277. [Epub ahead of print]

Lujanieneo G., Plukis A., Kimtys E., Remeikis V., Jankunaiteo D., Ogorodnikov B. I. Study of ^{137}Cs, ^{90}Sr, $^{239,240}Pu$, ^{238}Pu and ^{241}Am behavior in the Chernobyl soil. // Journal of Radioanalytical and Nuclear Chemistry, Vol. 251, No. 1 (2002) 59–68.

Mauring, A., Gäfvert, T., Drefvelin, J., Aleksandersen, T., Møller, B., 2014. Calibration of HPGe detectors for in situ gamma spectrometry at the Norwegian Radiation Protection Authority: Method, results and validation. Technical document no. 3. Østerås: Norwegian Radiation Protection Authority. (Language: Norwegian)

Menge, P.R., Gautier, G., Iltis, A., Rozsa, C., Solovyev, V., 2007, Performance of large lanthanum bromide scintillators. Nucl Instrum Methods 579:6DOI: 10.1016/j.nima.2007.04.002

Sowa W., Martini E., Gehrcke K., Marschner P., Naziry M. J., 1989. Uncertainties of in situ gamma spectrometry for environmental monitoring. Radiat. Prot. Dosim. 27, 93-101.

Zombori, P., Andrasi, A., Nemeth, I. A new method for the determination of radionuclide distribution in the soil by in situ gamma-ray spectrometry. Report KFKI-1992-20/K, Hungarian Academy of Science, Central Research Institute for Physics, Budapest; 1992.